INFRARED PHENOMENA IN QUANTUM ELECTRODYNAMICS

W. VAN HAERINGEN

INFRARED PHENOMENA IN QUANTUM ELECTRODYNAMICS

PROEFSCHRIFT

TER VERKRIJGING VAN DE GRAAD VAN DOCTOR IN DE WIS- EN NATUURKUNDE AAN DE RIJKSUNIVERSITEIT TE UTRECHT, OP GEZAG VAN DE RECTOR MAGNIFICUS DR. J. F. NUBOER, HOOGLERAAR IN DE FACULTEIT DER GENEESKUNDE, VOLGENS BESLUIT VAN DE SENAAT DER UNIVERSITEIT TEGEN DE BEDENKINGEN VAN DE FACULTEIT DER WIS- EN NATUURKUNDE TE VERDEDIGEN OP MAANDAG 27 JUNI 1960 DES NAMIDDAGS TE 2.45 UUR PRECIES

DOOR

WILLEM VAN HAERINGEN

GEBOREN TE BERGEN OP ZOOM

Promotor: PROF. DR. L. CH. P. VAN HOVE

Aan mijn moeder
Aan de nagedachtenis van mijn vader
Aan mijn vrouw en kinderen

CONTENTS

Chapter I

THE PHYSICAL ONE-ELECTRON STATES IN THE INFRARED REGION

Synopsis

In view of remaining obscurities and difficulties in existing treatments of the infrared divergences in quantum electrodynamics this problem has been considered anew. The approximate model introduced in 1937 by Bloch and Nordsieck is rediscussed. It is explicitly shown to be a good substitute for the complete theory as long as one restricts oneself to infrared radiation. A non-covariant diagram technique is used to prove that neglect of recoil and pair effects is indeed allowed in the infrared radiation range. The effects of vacuum polarization and charge renormalization require special attention. They are treated in second order with the regularization method of Pauli and Villars.

1. *Introduction.* The present investigation is devoted to quantum electrodynamics in the electromagnetic wavelength range large compared to the Compton wavelength $\hbar/mc$ of the electron. This range is often called the infrared (i.r.) region. As is well known special difficulties are arising in the i.r. region as a consequence of the vanishing rest mass of the electromagnetic quanta (photons). In particular they lead to divergent integrals in the perturbation expansion of radiative corrections originating from the i.r. region. In contradistinction to the divergences coming from the ultraviolet (short) wavelength range the i.r. divergences cannot be eliminated by means of the well known renormalization method of quantum electrodynamics.

The fundamental contribution to the solution of the i.r. difficulties was made by Bloch and Nordsieck [1]). They treated a simplified model of electrodynamics in which pair effects and recoil of the electron are neglected and noticed that this model is a good substitute for the complete theory as long as one restricts oneself to i.r. radiation. This model is exactly solvable and leads to the insight that scattering processes are necessarily accompanied by the emission of unobservably weak radiation consisting of infinitely many quanta of very small total energy. This observation gives the key to the solution of the i.r. problem. The treatment of Bloch and Nordsieck, however, is far from complete. For instance it is a priori not clear to which extent the conclusions of these authors can be applied to the complete theory in which hard (short wavelength) radiation plays a role too.

A serious attempt to obtain a rigorous solution of all i.r. difficulties was undertaken by Jauch and Rohrlich [2]). In a relativistic covariant treatment they extend the work of Bloch and Nordsieck in the sense that radiative effects of all wavelengths are considered simultaneously. Feynman diagrams play a fundamental role in the analysis. By means of a very useful but not quite clearly defined concept of 'basic diagram', Jauch and Rohrlich readily obtain a generalization of Bloch and Nordsieck's results. Although this work seemed at first sight to exhaust the i.r. problem it soon appeared that several questions required further study. The limits of validity of Jauch and Rohrlich's results were questioned by Lomon [3]), while Nakanishi [4]) noted that diagrams in which soft (i.e. very low frequency) photons are attached to internal lines, were disregarded without justification. Yennie and Suura [5]) used arguments similar to Jauch and Rohrlich's and showed more clearly the origin of the cancellation of i.r. divergences originating from soft real and virtual photons. None of these papers can be regarded as clarifying fully the complicated i.r. phenomena of electrodynamics *).

Aside from these different questions and investigations there is still another problem which concerns *Compton scattering* in the non relativistic limit (soft photons scattered on slow electrons). What does one find if one calculates for this process radiative corrections up to a given order? According to a theorem of Thirring [6]) all observable radiative corrections should vanish in the non relativistic limit, their only effect being the replacement of mass and charge by their renormalized values in the second order cross section formula (usually called the *Thomson formula*). However, when a finite order calculation is made the result turns out to be i.r. divergent in clear violation of the above theorem. As an example we quote Brown and Feynman's [7]) calculation of the cross section in sixth order in the charge. Obviously the theorem of Thirring should be amended so as to take soft photon effects properly into account.

In view of the afore mentioned difficulties it was considered worthwhile to devote a new detailed investigation to the problem of the i.r. divergences in quantum electrodynamics. The method to be followed is closely inspired on the pioneering work of Bloch and Nordsieck but aims at including the whole photon spectrum. In line with Bloch and Nordsieck a non-covariant treatment will be adopted. The perturbation expansions will be based on the non-covariant perturbation formalism of Van Hove [8]) and Hugenholtz [9]). This formalism turns out to be well suited for the treatment of the problem in question. This manifests itself most clearly in the non-covariant

*) Both D. R. Yennie and E. L. Lomon have been engaged lately in a new study of the i.r. difficulties in quantum electrodynamics (private communication to L. Van Hove).

diagram technique, which enables us to split off i.r. divergent effects directly. In addition our work provides a concrete application of this formalism to an interesting aspect of low energy quantum electrodynamics. As is usually done in i.r. studies we concentrate entirely on the transversely polarized components of the electromagnetic field. The main lines of this investigation will be as follows. We consider first electrodynamics with a very low cut off ($\hbar\bar{\omega} \ll mc^2$) and we ask how well this system is approximated by the model of Bloch and Nordsieck. One verifies in succession that recoil and pair effects can be neglected in the low frequency region. Pair effects form the least trivial and most interesting point in this connection, due to the fact that even for a very low photon cut off they give rise to vacuum polarization and charge renormalization. The treatment of electrodynamics with a low cut off will be the main object of the present article. In the following article we then study within the framework of full quantum electrodynamics two concrete scattering processes with all i.r. aspects connected to them. We select *bremsstrahlung* and *Compton scattering*, the latter process because of its relation to the theorem of Thirring [6]) mentioned before. In the treatment of these scattering processes we shall make extensive use of diagrams in the non-covariant formalism and shall often rely on the arguments of the present paper.

We start in the next section with the treatment of the Bloch-Nordsieck model. The corresponding eigenvalue problem is solved by a method different from Bloch and Nordsieck's, and more directly susceptible of extension to the complete theory. We give explicit expressions for the physical one-electron states expanded in unperturbed states. In section 3 we start the discussion of the range of validity of the model by investigating the nature and order of magnitude of all effects neglected. The complications due to the self-energy of the photon are treated separately in section 4, which makes essential use of the regularization method of Pauli and Villars [10]).

2. *The Bloch-Nordsieck model.* Bloch and Nordsieck studied the interaction between a classical current distribution and the transverse electromagnetic field with the aid of the hamiltonian *)

$$H_B = (\boldsymbol{\mu}, \boldsymbol{p} - \Sigma_{s\lambda}\, \boldsymbol{a}_{s\lambda}\, [P_{s\lambda} \cos(\boldsymbol{k}_s, \boldsymbol{r}) + Q_{s\lambda} \sin(\boldsymbol{k}_s, \boldsymbol{r})]) + \\ + m(1 - \mu^2)^{\frac{1}{2}} + \tfrac{1}{2} \Sigma_{s\lambda} (P_{s\lambda}{}^2 + Q_{s\lambda}{}^2)\, \omega_s, \qquad (2.1)$$

where $\boldsymbol{a}_{s\lambda} = 2e(\pi/\Omega\omega_s)^{\frac{1}{2}}\, \boldsymbol{\varepsilon}_{s\lambda}$ and $(\boldsymbol{\varepsilon}_{s\lambda}, \boldsymbol{k}_s) = 0$. The electromagnetic wave vector $\boldsymbol{k}_s$ runs over the points of an infinite cubic lattice in momentum space with a lattice spacing $2\pi\Omega^{-\frac{1}{3}}$; Ω is the volume of the cube in which the system is enclosed with the usual periodic boundary conditions; Σ_λ is a summation over the two transverse polarizations of the electromagnetic

*) We use units so that $\hbar = c = 1$.

waves, $\boldsymbol{\varepsilon}_{s\lambda}$ being a unit vector in the direction of polarization; $\boldsymbol{p} = -i\partial/\partial\boldsymbol{r}$; $P_{s\lambda} = -i\partial/\partial Q_{s\lambda}$; $\omega_s = |\boldsymbol{k}_s|$ is the circular frequency of the wave with propagation vector $\boldsymbol{k}_s$; $\boldsymbol{\mu}$ is the velocity vector replacing the Dirac $\boldsymbol{\alpha}$ matrices. The difference with complete quantum electrodynamics is the replacement of the Dirac matrix fourvector $(\boldsymbol{\alpha}, \beta)$ by $(\boldsymbol{\mu}, (1-\mu^2)^{\frac{1}{2}})$. As noticed by Bloch and Nordsieck and confirmed below such a replacement is allowed if only photons of low energy are considered in the interaction; we therefore expect to obtain from a study of (2.1) valuable information on the infrared difficulties of quantum electrodynamics.

The eigenvalue problem

$$H_B f(\boldsymbol{r}, Q_{s\lambda}) = E f(\boldsymbol{r}, Q_{s\lambda}) \tag{2.2}$$

is exactly solvable. Bloch and Nordsieck obtain the solution by means of a suitable canonical transformation. Here another method is followed, more convenient for later extension to full electrodynamics. We first introduce creation and destruction operators for the electromagnetic and electron fields. The creation operator $c_{s\lambda}{}^*$ and the destruction operator $c_{s\lambda}$ for a photon with propagation vector $\boldsymbol{k}_s$ and polarization λ are given by

$$-ic_{s\lambda}{}^* = 2^{-\frac{1}{2}}(P_{s\lambda} + iQ_{s\lambda}) \tag{2.3a}$$

$$+ic_{s\lambda} = 2^{-\frac{1}{2}}(P_{s\lambda} - iQ_{s\lambda}). \tag{2.3b}$$

It is easily verified that

$$[c_{s\lambda}, c_{s'\lambda'}{}^*] = \delta_{ss'}\,\delta_{\lambda\lambda'};\ [c_{s\lambda}, c_{s'\lambda'}] = [c_{s\lambda}{}^*, c^*{}_{s'\lambda'}] = 0. \tag{2.4}$$

We write $H_B = H_B{}^{0\prime} + V_B{}'$ with

$$H_B{}^{0\prime} = -\,i(\boldsymbol{\mu}, \partial/\partial\boldsymbol{r}) + m(1-\mu^2)^{\frac{1}{2}} + \Sigma_{s\lambda}\omega_s c_{s\lambda}{}^* c_{s\lambda} \tag{2.5a}$$

$$V_B{}' = 2^{-\frac{1}{2}}i(\boldsymbol{\mu}, \Sigma_{s\lambda}\boldsymbol{a}_{s\lambda}[c_{s\lambda}{}^*\, e^{-i(\boldsymbol{k}_s, \boldsymbol{r})} - c_{s\lambda}\, e^{i(\boldsymbol{k}_s, \boldsymbol{r})}]). \tag{2.5b}$$

In (2.5a) we omitted the zero-point energy of the electromagnetic field $\frac{1}{2}\Sigma_{s\lambda}\omega_s$.

The general solution of

$$[-\,i(\boldsymbol{\mu}, \partial/\partial\boldsymbol{r}) + m(1-\mu^2)^{\frac{1}{2}}]\,\psi(\boldsymbol{r}) = E\psi(\boldsymbol{r}) \tag{2.6}$$

with periodic boundary conditions on the surface of the cube with volume Ω is

$$\psi(\boldsymbol{r}) = \Sigma_{\boldsymbol{p}}\,\Omega^{-\frac{1}{2}} b(\boldsymbol{p})\, e^{i(\boldsymbol{p}, \boldsymbol{r})}, \tag{2.7}$$

the sum running over the same momentum values as $\boldsymbol{k}_s$. By taking the coefficients $b(\boldsymbol{p})$, $b^*(\boldsymbol{p})$ as operators with the usual anti-commutation rules

$$\{b(\boldsymbol{p}), b^*(\boldsymbol{p}')\} = \delta_{\boldsymbol{p}\boldsymbol{p}'};\ \{b(\boldsymbol{p}), b(\boldsymbol{p}')\} = \{b^*(\boldsymbol{p}), b(\boldsymbol{p}')\} = 0 \tag{2.8}$$

and by putting

$$[c_{s\lambda}, b(\boldsymbol{p})] = [c_{s\lambda}, b^*(\boldsymbol{p})] = 0;\ [c_{s\lambda}{}^*, b(\boldsymbol{p})] = [c_{s\lambda}{}^*, b^*(\boldsymbol{p})] = 0, \tag{2.9}$$

we get after this second quantization of the classical current field

$$H_B^{0''} = \Sigma_p\{(\boldsymbol{\mu}, \boldsymbol{p}) + m(1 - \mu^2)^{\frac{1}{2}}\}b^*(\boldsymbol{p})\, b(\boldsymbol{p}) + \Sigma_{s\lambda}\, \omega_s c_{s\lambda}{}^* c_{s\lambda} \tag{2.10a}$$

$$V_B'' = \Sigma_{ps\lambda}\, 2^{-\frac{1}{2}} i(\boldsymbol{\mu}, \boldsymbol{a}_{s\lambda})\, b^*(\boldsymbol{p})\, b(\boldsymbol{p} + \boldsymbol{k}_s)\{c_{s\lambda}{}^* - c_{-s\lambda}\}, \tag{2.10b}$$

where $c_{-s\lambda}$ destroys a photon with propagation vector—$\boldsymbol{k}_s$. As verified later the electron self-energy due to the interaction with the electromagnetic field is

$$\delta E'(\boldsymbol{p}) = -\tfrac{1}{2}\Sigma_{s\lambda}(\boldsymbol{\mu}, \boldsymbol{a}_{s\lambda})^2/(\omega_s - (\boldsymbol{\mu}, \boldsymbol{k}_s)). \tag{2.11}$$

Therefore we rewrite finally H_B as $H_B = H_B{}^0 + V_B$ with

$$H_B{}^0 = H_B{}^{0''} + \Sigma_p\, \delta E'(\boldsymbol{p})\, b^*(\boldsymbol{p})\, b(\boldsymbol{p}) \tag{2.12a}$$

$$V_B = V_B'' - \Sigma_p\, \delta E'(\boldsymbol{p})\, b^*(\boldsymbol{p})\, b(\boldsymbol{p}). \tag{2,12b}$$

Let $|\boldsymbol{p};\ \{m_{s\lambda}\}\rangle = b^*(\boldsymbol{p})\ \Pi_{s\lambda}(m_{s\lambda}!)^{-\frac{1}{2}} c^{*m_{s\lambda}}_{s\lambda}\, |0\rangle$ be the normalized one-electron solutions of

$$(H_B{}^0 - E)\, |\alpha\rangle = 0, \tag{2.13}$$

$|0\rangle$ being the normalized unperturbed vacuum state ($\langle 0|0\rangle = 1$). The photon numbers $m_{s\lambda}$ are non negative integers. The normalized one-electron solutions of

$$(H_B - E)\, |\alpha) = 0 \tag{2.14}$$

can be written formally as [11])

$$\begin{aligned} |\boldsymbol{p};\{m_{s\lambda}\})_\mu = N^{\frac{1}{2}}_{\boldsymbol{p};\{m_{s\lambda}\}}\, [|\boldsymbol{p};\{m_{s\lambda}\}\rangle + \Sigma_{\{n_{s\lambda}\}}\langle \boldsymbol{p} + \Sigma_{s\lambda}(m_{s\lambda} - n_{s\lambda})\boldsymbol{k}_s;\ \{n_{s\lambda}\}|\\ \{\Sigma_{l=1}^{\infty}(-D_B{}^0(E'(\boldsymbol{p}) + \Sigma_{s\lambda}\,\omega_s m_{s\lambda})V_B)^l\}_{n.i.}\, |\boldsymbol{p};\{m_{s\lambda}\}\rangle\\ |\boldsymbol{p} + \Sigma_{s\lambda}(m_{s\lambda} - n_{s\lambda})\boldsymbol{k}_s;\ \{n_{s\lambda}\}\rangle \end{aligned} \tag{2.15}$$

where $D_B{}^0(z) = (H_B{}^0 - z)^{-1}$ and $N_{\boldsymbol{p};\{m_{s\lambda}\}}$ is a normalization constant; further $E'(\boldsymbol{p}) = (\boldsymbol{\mu}, \boldsymbol{p}) + m(1 - \mu^2)^{\frac{1}{2}} - \delta E'(\boldsymbol{p})$. By *n.i.* is meant that all intermediate states and the final state are non-initial, i.e. different from the initial state $|\boldsymbol{p};\{m_{s\lambda}\}\rangle$. This formula is valid for arbitrary interaction V_B.

The coefficients (i.e. the matrix elements) of the unperturbed (bare particle) states in (2.15) are easily found with the aid of diagrams. In these diagrams an electron is represented by a full line, a photon by a dotted one. The operator V_B'' acts in the vertices, the operator $-\Sigma_p\, \delta E'(\boldsymbol{p})b^*(\boldsymbol{p})b(\boldsymbol{p})$ acts in the points marked with a cross and further denoted as δE-points, and finally the operator $D_B{}^0(z)$ must be taken in all intermediate states as well as in the final state which is on the left of the diagram. The diagrams are read from right to left.

It can be proved that in the matrix elements of (2.15) all contributions of diagrams with internal photon lines and/or δE-corrections exactly cancel each other.

The proof runs as follows: Start from a certain diagram M, contributing to some matrix element in (2.15), in which internal photon lines and δE-points may occur.

Insert in M in all possible ways one internal photon line or one δE-point. In this way one gets a set of diagrams representing the whole second order correction to M. We prove that this correction vanishes. Let the diagram M be represented by fig. 1 in which each point is either a vertex or a δE-point. We omit all photon lines in M because they are irrelevant for the argument.

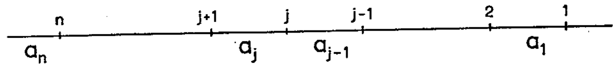

Fig. 1. Diagram M (the photon lines are not drawn). The points are either vertices or δE-points. The a's denote the energy denominators.

Let a_i be the i^{th} energy denominator in M (going from right to left). Now consider the diagrams of fig. 2, which form a subclass of the set mentioned above.

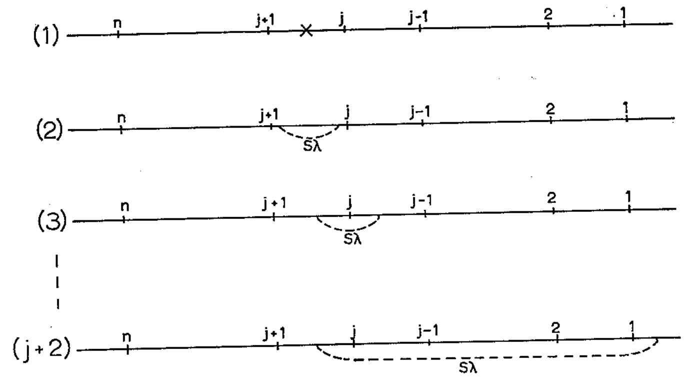

Fig. 2. Subclass of diagrams contributing to the second order correction to diagram M.

Write $\omega_s - (\boldsymbol{\mu}, \boldsymbol{k}_s) = b$, where s refers to the photon line in the figure. If we omit all summations and also the factor $\Pi_{i=1}^{n} L_i(\boldsymbol{\mu}, \boldsymbol{a}_{s\lambda})^2/2$ where

$$L_i = \begin{cases} \pm\, 2^{-\frac{1}{2}}\, i(\boldsymbol{\mu}, \boldsymbol{a}_{s_i\lambda_i}) \text{ if the } i^{th} \text{ point is a vertex} \\ \frac{1}{2}\Sigma_{s'\lambda'}\ (\boldsymbol{\mu}, \boldsymbol{a}_{s'\lambda'})^2/(\omega_{s'} - (\boldsymbol{\mu}, \boldsymbol{k}_{s'})) \text{ if the } i^{th} \text{ point is a } \delta E\text{-point,} \end{cases}$$

the diagrams (2), (3) ... (j + 2) contribute together

$$\frac{1}{\Pi_{i=1}^{n} a_i}\left[\frac{1}{a_j(a_j+b)} + \frac{a_j}{a_j(a_j+b)(a_{j-1}+b)} + \ldots + \frac{a_j a_{j-1} \ldots a_1}{a_j(a_j+b)(a_{j-1}+b) \ldots (a_1+b)b}\right] = \frac{1}{\Pi_{i=1}^{n} a_i} \cdot \frac{1}{a_j b}\,.$$

However in view of (2.11) the diagram (1) contributes

$$-\frac{1}{\Pi_{i=1}^{n} a_i} \cdot \frac{1}{a_j b}\,.$$

So the total contribution of the diagrams in fig. 2 vanishes and as this result is independent of j the whole second order correction to M vanishes. From this we conclude that we can forget all diagrams containing internal photon lines and/or δE-points.

This conclusion allows us to find in closed form the explicit expression of the matrix elements in (2.15), for the remaining number of diagrams contributing to them is finite. One obtains

$$|\boldsymbol{p};\{m_{s\lambda}\})_\mu = \overline{N}_\mu^{\frac{1}{2}} \Sigma_{\{n_{s\lambda}\}} \Pi_{s\lambda}(-2^{-\frac{1}{2}} i\, \sigma_{\mu s\lambda})^{|n_{s\lambda}-m_{s\lambda}|} \; (m_{s\lambda}!\, n_{s\lambda}!)^{\frac{1}{2}}$$

$$\Sigma_{\zeta=0}^{s\lambda} (-\tfrac{1}{2}\sigma^2_{\mu s\lambda})^\zeta/(l_{s\lambda}-\zeta)!\,\zeta!(|n_{s\lambda}-m_{s\lambda}|+\zeta)!|\, \boldsymbol{p}+\Sigma_{s\lambda}(m_{s\lambda}-n_{s\lambda})\boldsymbol{k}_s;\{n_{s\lambda}\}\rangle, \quad (2.16)$$

where $\Sigma_{\{n_{s\lambda}\}}$ is a summation over all possible sets of photons;

$l_{s\lambda} = \min.(n_{s\lambda}, m_{s\lambda})$ and

$$\sigma_{\mu s\lambda} = (\boldsymbol{\mu}, \boldsymbol{a}_{s\lambda})/(\omega_s - (\boldsymbol{\mu}, \boldsymbol{k}_s)) \quad (2.16a)$$

$$\overline{N}_\mu = \exp[-\tfrac{1}{2}\Sigma_{s\lambda}\sigma^2_{\mu s\lambda}]. \quad (2.16b)$$

If $\Omega \to \infty$, the sum in the exponential becomes an integral divergent in the infrared as well as in the ultraviolet region.

In particular, for the one-electron state one finds

$$|\boldsymbol{p};\{0\})_\mu = \bar{O}_{\boldsymbol{p}}\,|0\rangle \quad (2.17)$$

$$\bar{O}_{\boldsymbol{p}} = \overline{N}_\mu^{\frac{1}{2}}\Sigma_{\{n_{s\lambda}\}}\Pi_{s\lambda}(-2^{-\frac{1}{2}}\, i\sigma_{\mu s\lambda})^{n_{s\lambda}}(n_{s\lambda}!)^{-1} b^*(\boldsymbol{p}-\Sigma_{s\lambda}n_{s\lambda}\boldsymbol{k}_s)\, c^{*\,n_{s\lambda}}_{s\lambda}. \quad (2.18)$$

Note that the above derivation confirms the value (2.11) of the electron self-energy. (2.16) is the result of Bloch and Nordsieck. From now on we only use solutions (2.16) in which $\boldsymbol{p}$ and $\boldsymbol{\mu}$ are related by $\boldsymbol{p} = m\boldsymbol{\mu}|(1-\mu^2)^{\frac{1}{2}}$, this meaning that the electron has velocity $\boldsymbol{\mu}$.

3. *Range of validity of the Bloch-Nordsieck model.* In quantum electrodynamics, if the electromagnetic field is restricted to the transverse components, the hamiltonian has the form

$$H = (\boldsymbol{\alpha}, \boldsymbol{p} - \Sigma_{s\lambda}\boldsymbol{a}_{s\lambda}[P_{s\lambda}\cos(\boldsymbol{k}_s, \boldsymbol{r}) + Q_{s\lambda}\sin(\boldsymbol{k}_s, \boldsymbol{r})]) + \beta m + \tfrac{1}{2}\Sigma_{s\lambda}(P_{s\lambda}^2 + Q_{s\lambda}^2)\omega_s \quad (3.1)$$

which becomes after second quantization

$$H = H_0 + V, \quad (3.2)$$

with

$$H_0 = \Sigma_{pr}\,\varepsilon(\boldsymbol{p})[b_r^*(\boldsymbol{p})\, b_r(\boldsymbol{p}) + d_r^*(\boldsymbol{p})\, d_r(\boldsymbol{p})] + \Sigma_{s\lambda}\,\omega_s\, c_{s\lambda}^* c_{s\lambda}, \quad (3.2a)$$

$$V = \Sigma_{prr's\lambda}\, im(2\varepsilon(\boldsymbol{p})\,\varepsilon(\boldsymbol{p}+\boldsymbol{k}_s))^{-\frac{1}{2}}[b_r^*(\boldsymbol{p})w_r^*(\boldsymbol{p}) + d_r(-\boldsymbol{p})\, v_r^*(-\boldsymbol{p})]$$

$$(\boldsymbol{\alpha}, \boldsymbol{a}_{s\lambda})[b_{r'}(\boldsymbol{p}+\boldsymbol{k}_s)\, w_{r'}(\boldsymbol{p}+\boldsymbol{k}_s) + d_{r'}^*(-\boldsymbol{p}-\boldsymbol{k}_s)v_{r'}(-\boldsymbol{p}-\boldsymbol{k}_s)][c_{s\lambda}^* - c_{-s\lambda}]. \quad (3.2b)$$

Most of the notation has been defined previously. $\boldsymbol{\alpha}$, β are the Dirac matrices and $\varepsilon(\boldsymbol{p}) = (m^2 + \boldsymbol{p}^2)^{\frac{1}{2}}$ is the unrenormalized electron energy. The operators $d_r(\boldsymbol{p})$, $d_r^*(\boldsymbol{p})$ destroy and create the positrons. The indices r, r' indicate the spin orientation of electrons and positrons. The spinor notation is the same as in reference 12.

The physical state of the electron with momentum $\boldsymbol{p}$ and spin r can formally be written as [11])

$$|\boldsymbol{p}_r; \{0\}) = O_{pr}\, |0) \tag{3.3}$$

$$O_{pr} = N_p^{\frac{1}{2}}[b_r^*(\boldsymbol{p}) + \Sigma_\alpha \Sigma_\delta \langle\alpha|\{\Sigma_{j=1}^{\infty}(-D^0(E(\boldsymbol{p}))V)^j_{n.i.}\}_\delta\, |\boldsymbol{p}_r;\{0\}\rangle\, A^*(\alpha)] \tag{3.4}$$

where $|0)$ is the normalized physical vacuum state; Σ_δ is a summation over connected diagrams; the index *n.i.* has the same meaning as in (2.15); $|\alpha\rangle$ are the normalized eigenstates of H_0; the operator $A^*(\alpha)$ creates $|\alpha\rangle$ from the bare vacuum $|0\rangle$; $D^0(E(\boldsymbol{p})) = (H_0 - E(\boldsymbol{p}))^{-1}$; $E(\boldsymbol{p})$ is the difference in energy between the states $|\boldsymbol{p}_r; \{0\})$ and $|0)$; N_p is a normalization constant, given by

$$N_p = (1 + ((\partial/\partial l)\, G_{\boldsymbol{p}}(l))_{l=E(\boldsymbol{p})})^{-1} \tag{3.5}$$

where

$$G_\alpha(l) = \langle\alpha|[-V + VD(l)V - VD(l)VD(l)V + \ldots]_{idc}\, |\alpha\rangle. \tag{3.6}$$

In (3.6) $D(l)$ is the diagonal part of the resolvent operator $R(l) = (H - l)^{-1}$; the subscript *idc* means that only contributions of irreducible connected diagrams should be taken *).

Let us introduce for the photons a very low cut off $\bar{\omega}$, verifying $\bar{\omega} \ll m$. Then it is our contention that the physical one-electron state (3.3) can be approximated by $\bar{O}_{pr}\, |0)$, where $\bar{O}_{pr}$ is, except for the spin, the same operator as in (2.18), i.e.

$$\bar{O}_{pr} = \bar{N}_p^{\frac{1}{2}}\, \Sigma_{\{n_{s\lambda}\}}\, \Pi_{s\lambda}(-2^{-\frac{1}{2}}i\sigma_{\mu s\lambda})^{n_{s\lambda}}(n_{s\lambda}!)^{-1} b_r^*(\boldsymbol{p} - \Sigma_{s\lambda} n_{s\lambda}\boldsymbol{k}_s)\; c^{*\;n_{s\lambda}}_{s\lambda}. \tag{3.7}$$

The difference between O_{pr} and $\bar{O}_{pr}$ mathematically originates from two facts. The class of diagrams contributing to (3.4) is much larger than the corresponding class for (3.7); this is due to pair creation and annihilation terms. Moreover, identical diagrams give different contributions, the difference being the neglect of the electron's recoil in (3.7). So we have to show that pair effects as well as recoil effects become unimportant if $\bar{\omega}$ is small enough.

Let us rewrite (3.4) and (3.7) in abbreviated form

$$\begin{aligned} O_{pr} &= N_p^{\frac{1}{2}}[b_r^*(\boldsymbol{p}) + \Sigma_\alpha C_\alpha A^*(\alpha)] \\ \bar{O}_{pr} &= \bar{N}_p^{\frac{1}{2}}[b_r^*(\boldsymbol{p}) + \Sigma_\alpha \bar{C}_\alpha A^*(\alpha)]. \end{aligned} \tag{3.8}$$

We want to show

$$\Sigma_\alpha |C_\alpha - \bar{C}_\alpha|^2 = \mathrm{O}(e^2\bar{\omega}/m)\, \Sigma_\alpha |\bar{C}_\alpha|^2 \tag{3.9}$$

if $\bar{\omega}/m \ll 1$ and $e^2\bar{\omega}/m \ll 1$. The charge e is the unrenormalized one, but our statement is only true if the renormalized charge e' is equal to the unrenormalized one, as we shall see in section 4. In practice, since $e^{-2} \simeq 137$ the condition $e^2\bar{\omega}/m \ll 1$ follows from $\bar{\omega}/m \ll 1$.

*) For the concept of irreducibility here used see Hugenholtz [9]), p. 494.

Let us first consider diagrams without pairs. The lowest order diagram which contributes to the left-hand sum in (3.9) is given in fig. 3. This contribution is $\frac{1}{2}\sum_{s\lambda}^{\varpi} \{\boldsymbol{\mu}, \boldsymbol{a}_{s\lambda})^2/(\omega_s - (\boldsymbol{\mu}, \boldsymbol{k}_s))^2\} \mathrm{O}(\omega_s/E(\boldsymbol{p})) =$ $= \mathrm{O}(e^2\bar{\omega}/m)$ if $\bar{\omega}/m \ll 1$. The lowest order corrections (without pairs) to fig. 3 are represented by fig. 4.

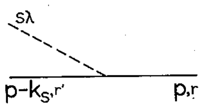

Fig. 3. Lowest order diagram contributing to $\Sigma_\alpha |C_\alpha - \bar{C}_\alpha|^2$.

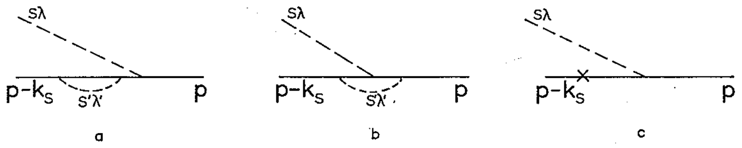

Fig. 4. All second order corrections to fig. 3 without pairs.

As we found in the preceding section these diagrams give a vanishing contribution to the coefficients $\bar{C}_\alpha$. When calculating the coefficients C_α, the contribution of the δE-point (cross) in fig. 4 is no longer given by (2.11) but by the electron self-energy in the full theory with cut off $\bar{\omega}$. We here include that part of the self-energy which originates from the diagram in fig. 5*a* (the part originating from fig. 5*b* is included later on).

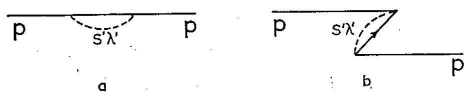

Fig. 5. Second order electron self-energy diagrams.

By so doing one finds for the second order correction to fig. 3 a contribution of relative order $e^2\bar{\omega}/m$ if $\bar{\omega}/m \ll 1$; higher order corrections to fig. 3 are found to be of the same order. When discussing diagrams without virtual photons or δE-points, with more than one external photon line, one finds similarly that the contribution to $\sum_\alpha |C_\alpha - \bar{C}_\alpha|^2$ equals $\mathrm{O}(e^2\bar{\omega}/m)\{\frac{1}{2}\sum_{s\lambda}^{\varpi}\sigma^2_{\mu s\lambda}\}^{n-1}/(n-1)!$ if n is the number of external photon lines and if $\bar{\omega}/m \ll 1$. Radiative corrections to these diagrams are again of order $e^2\bar{\omega}/m$. Restricting us to diagrams without pairs we find in this way

$$\sum_\alpha |C_\alpha - \bar{C}_\alpha|^2 = \mathrm{O}(e^2\bar{\omega}/m)\exp[\tfrac{1}{2}\textstyle\sum_{s\lambda}^{\varpi}\sigma^2_{\mu s\lambda}], \tag{3.10}$$

where

$$\exp[\tfrac{1}{2}\textstyle\sum_{s\lambda}^{\varpi}\sigma^2_{\mu s\lambda}] = \bar{N}_p^{-1} = \sum_\alpha |\bar{C}_\alpha|^2. \tag{3.11}$$

Now consider diagrams with pairs. The contribution to $\sum_\alpha |C_\alpha - \bar{C}_\alpha|^2$ originating from the diagram of fig. 6*a* turned out to be $\mathrm{O}(e^2\bar{\omega}/m)\,\frac{1}{2}\sum_{s\lambda}^{\varpi}\sigma^2_{\mu s\lambda}$.

This result is not affected by the diagram in fig. 6*b*. Although the vertex factors of fig. 6*b* are of order 1 in contradistinction to those in fig. 6*a*, which are of order $\mu = v/c$, the fact that the latter diagram has one small denominator less dominates in such a way that its contribution can be neglected compared to the contribution of fig. 6*a*. One easily extends this result to diagrams with more external photon lines; quite generally, as long as there are no virtual photons or δE-points one can neglect all diagrams in which the electron line is not straight, i.e. in which the initial electron annihilates with a positron.

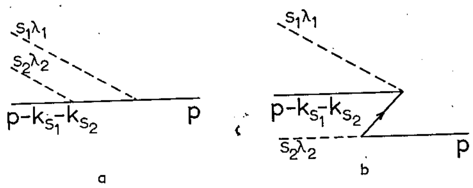

Fig. 6. Second order diagrams contributing to $\Sigma_\alpha |C_\alpha - \overline{C}_\alpha|^2$.

The situation is different when virtual effects are present. Fig. 7*a* gives an example of a diagram in which pair effects give rise to an additional small energy denominator. This diagram is however compensated in the limit $\omega_s \to 0$ by the diagram of fig. 7*b* where the cross contributes the part of the self-energy corresponding to the diagram in fig. 5*b*.

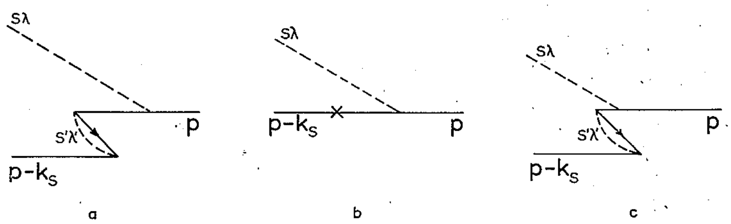

Fig. 7. Second order corrections to fig. 3 with pairs.

This is true except for contributions of relative order $e^2\bar{\omega}/m$. The diagram in fig. 7*c* and similar diagrams can be neglected because of two large energy denominators. They give rise to corrections to the diagram of fig. 3 which are of relative order $e^2\bar{\omega}/m$.

Finally we have to deal with diagrams in which the photon self-energy plays a role, i.e. diagrams where photons create pairs. In fig. 8 for instance all second order corrections to fig. 3 involving such effects are represented.

In fig. 9 the lowest order diagrams are represented with pairs in the final state. It will be shown in the next section that the error made by neglecting them is of order $e^2\bar{\omega}/m$ if the renormalized charge is equal to the unrenormalized one, a result which can be extended to higher orders.

At first sight the diagrams now considered seem to give rise to highly divergent integrals over $\boldsymbol{k}_s$ in the infrared region; for instance in fig. 9*a* the contribution to $\sum_\alpha |C_\alpha - \bar{C}_\alpha|^2$ is proportional to $\int_0^\infty \mathrm{d}\omega_s/\omega_s^2$. In addition the integration over $\boldsymbol{p}'$ becomes linearly divergent for large $\boldsymbol{p}'$. In the case of fig. 8*a* the integration over the virtual pair turns out to be even quadratically

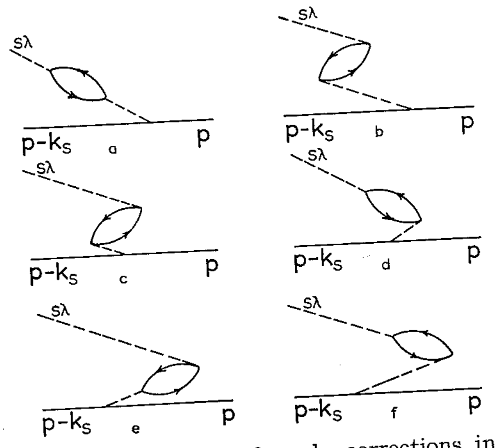

Fig. 8. Second order corrections to fig. 3; only corrections in the photon line are considered.

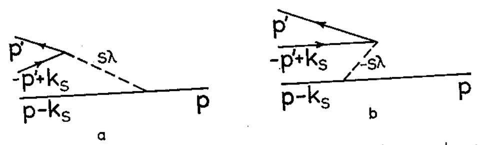

Fig. 9. Lowest order diagrams contributing to matrix elements with pairs in the final state.

divergent. The problems arising here are all connected with the photon self-energy. We must deal with them in some detail in order to complete our proof of (3.9). At the same time we shall point out and correct an error in the discussion of the physical photon state by Frazer and Van Hove in their paper on the stationary states of interacting fields [11]).

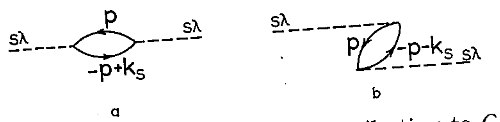

Fig. 10. Second order diagrams contributing to $G_{s\lambda}(l)$.

4. *The dressed photon. Photon self-energy. Charge renormalization.* The function $G_{s\lambda}(l)$ for the one-photon state $|0; s\lambda\rangle$, defined in analogy with (3.6) enables us to compute the photon self-energy $\delta\omega_s = -(G_{s\lambda}(l))_{l=\omega_s}$ (ω_s = observed frequency), and the normalization constant $N_{s\lambda}$ defined in analogy

with (3.5). We do this to second order. There are two second order diagrams contributing to $G_{s\lambda}(l)$ (fig. 10*ab*).
Their joined contribution turns out to be

$$G_{s\lambda}^{(2)}(l) = \Sigma_{prr'} \Bigg[\frac{m^2}{2E(\boldsymbol{p})E(-\boldsymbol{p}+\boldsymbol{k}_s)} \cdot \\ \cdot \frac{v_r^*(-\boldsymbol{p}+\boldsymbol{k}_s)(\boldsymbol{\alpha}, \boldsymbol{a}_{s\lambda})w_{r'}(\boldsymbol{p})w_{r'}^*(\boldsymbol{p})(\boldsymbol{\alpha},\boldsymbol{a}_{s\lambda})v_r(-\boldsymbol{p}+\boldsymbol{k}_s)}{E(\boldsymbol{p})+E(-\boldsymbol{p}+\boldsymbol{k}_s)-l} + \\ + \frac{m^2}{2E(\boldsymbol{p})\,E(-\boldsymbol{p}-\boldsymbol{k}_s)} \cdot \\ \cdot \frac{v_r^*(-\boldsymbol{p}-\boldsymbol{k}_s)(\boldsymbol{\alpha}, \boldsymbol{a}_{s\lambda})w_{r'}(\boldsymbol{p})w_{r'}^*(\boldsymbol{p})(\boldsymbol{\alpha}, \boldsymbol{a}_{s\lambda})\, v(-\boldsymbol{p}-\boldsymbol{k}_s)}{E(\boldsymbol{p})+E(-\boldsymbol{p}-\boldsymbol{k}_s)+2\omega_s-l} \Bigg]. \quad (4.1)$$

After computing the spinor sums one finds *)

$$G_s^{(2)}(l) = e^2\omega_s^{-1}\,[f(\boldsymbol{k}_s, l) + f(\boldsymbol{k}_s, l-2\omega_s)], \quad (4.2)$$

where

$$f(\boldsymbol{k}_s, l) = 2\pi\Omega^{-1}\,\Sigma_p \frac{m^2 + E(\boldsymbol{p})\,E(\boldsymbol{p}-\boldsymbol{k}_s) - (\boldsymbol{p}, \boldsymbol{k}_s) + (\boldsymbol{p}, \boldsymbol{k}_s)^2/\omega_s^2}{E(\boldsymbol{p})\,E(\boldsymbol{p}-\boldsymbol{k}_s)(E(\boldsymbol{p})+E(\boldsymbol{p}-\boldsymbol{k}_s)-l)}. \quad (4.3)$$

The summation over $\boldsymbol{p}$ is quadratically divergent at high $\boldsymbol{p}$ values. We treat the ultraviolet divergences of this type with the regularization prescription of Pauli and Villars [10]), consisting in the introduction, in a Lorentz and gauge invariant manner, of a sufficiently large number of auxiliary Fermi fields with complex coupling constants.

The regularized function $f_R(\boldsymbol{k}_s, l)$ is defined by

$$f_R(\boldsymbol{k}_s, l) = 2\pi\Omega^{-1}\,\Sigma_p\,\Sigma_i\,c_i \frac{M_i^2 + E_i(\boldsymbol{p})\,E_i(\boldsymbol{p}-\boldsymbol{k}_s) + p_{k_s}^2 - (\boldsymbol{p}, \boldsymbol{k}_s)}{E_i(\boldsymbol{p})\,E_i(\boldsymbol{p}-\boldsymbol{k}_s)(E_i(\boldsymbol{p})+E_i(\boldsymbol{p}-\boldsymbol{k}_s)-l)} \quad (4.4)$$

with the conditions

$$\Sigma_i c_i = 0;\ \ \Sigma_i c_i M_i^2 = 0, \quad (4.5)$$

where

$M_0 = m;\ c_0 = 1;\ M_i > 0;\ E_i(\boldsymbol{p}) = (\boldsymbol{p}^2 + M_i^2)^{\frac{1}{2}};\ p_{k_s} = (\boldsymbol{p}, \boldsymbol{k}_s)/\omega_s.$

The auxiliary fields have masses M_i and coupling constants $c_i^{\frac{1}{2}}e$ ($i = 1,2,\ldots$). The formal regularization prescription is to use f_R instead of f and take the limit $M_i \to \infty$ ($i > 0$) under the restrictions (4.5) The conditions (4.5) are exactly those needed to ensure convergence of $(G_s^{(2)}(l))_{l=\omega_s}$. With the regularization prescription one finds zero for the photon self-energy **),

*) As expected $G_{s\lambda}^{(2)}(l)$ is independent of the polarization index λ. We omit the argument λ in the following.

**) See for instance Gupta's calculation [13]), where an equivalent regularization procedure is used.

in agreement with the fact that the unrenormalized and renormalized photon mass must be equal and zero. When ω_s and l are small compared with m we write for (4.4) under the conditions (4.5)

$$f_R(\boldsymbol{k}_s, l) = 2\pi\Omega^{-1}\Sigma_p \Sigma_i c_i(2E_i^3(\boldsymbol{p}))^{-1}[M_i^2 + E_i^2(\boldsymbol{p}) + p_{k_s}{}^2 - 2(\boldsymbol{p}, \boldsymbol{k}_s) + \tfrac{1}{2}\omega_s^2(1 - p_{k_s}{}^2/E_i^2(\boldsymbol{p}))][1 + l/2E_i(\boldsymbol{p}) + 3(\boldsymbol{p}, \boldsymbol{k}_s)/2E_i^2(\boldsymbol{p}) - \tfrac{1}{2}\omega_s^2(3/2E_i^2(\boldsymbol{p}) - 5p_{k_s}{}^2/E_i^4(\boldsymbol{p})) + l^2/4E_i^2(\boldsymbol{p}) + l(\boldsymbol{p}, \boldsymbol{k}_s)/E_i^3(\boldsymbol{p}) + \ldots]. \quad (4.6)$$

Since this expression depends only on the length ω_s of $\boldsymbol{k}_s$ we write $f_R(\boldsymbol{k}_s, l) = f_R(\omega_s, l)$. Further properties of this function are easily found from (4.6)

$$f_R(0, 0) = 0 \quad (4.7)$$

$$((\partial/\partial l)\, f_R(0, l))_{l=0} = -\tfrac{1}{8}\Sigma_i c_i M_i \quad (4.8)$$

$$((\partial/\partial \omega_s)\, f_R(\omega_s, 0))_{\omega_s=0} = 0 \quad (4.9)$$

$$((\partial^2/\partial l^2)\, f_R(0, l))_{l=0} = (1/3\pi)\, \Sigma_i c_i \ln M_0/M_i \quad (4.10)$$

$$((\partial/\partial \omega_s^2)\, f_R(\omega_s, 0))_{\omega_s=0} = -(1/6\pi)\, \Sigma_i c_i \ln M_0/M_i. \quad (4.11)$$

In this way we obtain the expansion

$$f_R(\omega_s, l) = f_R(0, 0) + (l/1!)((\partial/\partial l)\, f_R(0, l))_{l=0} + (l^2/2!)((\partial^2/\partial l^2)\, f_R(0, l))_{l=0} + (\omega_s^2/1!)(\partial/\partial \omega_s^2)\, f_R(\omega_s, 0))_{\omega_s=0} + \ldots = -\tfrac{1}{8}\, l\, \Sigma_i c_i M_i + (\omega_s^2 - l^2)(1/6\pi)\, \Sigma_i c_i \ln M_i/M_0 + \ldots \quad (4.12)$$

Among the unwritten terms in (4.12) those containing auxiliary masses and coupling constants vanish in the limit $M_i \to \infty$ $(i > 0)$. Only terms without auxiliary constants remain. The function $G_{Rs}{}^{(2)}(l)$ defined by the regularized righthand side of (4.2) is found to be for small ω_s and l

$$G_{Rs}{}^{(2)}(l) = e^2\omega_s^{-1}\{\tfrac{1}{4}(\omega_s - l)\, \Sigma_i c_i M_i - (\omega_s - l)^2(1/3\pi)\, \Sigma_i c_i \ln M_i/M_0 + \ldots\}. \quad (4.13)$$

The unwritten terms in the curly bracket of (4.13) have the order of magnitude

$$(\omega_s - l)\, m[O(\omega_s^2/m^2) + O(l\omega_s/m^2) + O(l^2/m^2)].$$

They depend on ω_s and l, not only on the difference $(\omega_s - l)$. The regularized normalization constant N_{Rs} is for small ω_s, to second order

$$N_{Rs}{}^{(2)} = (1 + ((\partial/\partial l)\, G_{Rs}{}^{(2)}(l))_{l=\omega_s})^{-1} = 1 + \tfrac{1}{4}e^2\omega_s^{-1}\, \Sigma_i c_i M_i + O\,(e^2\omega_s/m). \quad (4.14)$$

The expression (4.14) diverges for $\omega_s \to 0$ unless we put as an additional condition

$$\Sigma_i c_i M_i = 0. \quad (4.15)$$

When this is done we find

$$\lim_{\omega_s \to 0} N_{Rs}{}^{(2)} \equiv N_{R0}{}^{(2)} = 1. \quad (4.16)$$

The renormalization of the electric charge in the present non-covariant formulation will now be studied by considering the process of bremsstrahlung with the emission of a single soft photon. Virtual photon corrections on the electron line do not contribute to the charge renormalization as follows from the Ward identity [14] (which is also found to hold in the non-covariant formalism). We have to consider only the virtual pair corrections to the real photon line and we do this to second order. For low photon energy the charge renormalization will follow. We use the following expression of the S-matrix *).

$$\langle\alpha'|S|\alpha\rangle = \delta_{\mathrm{kr}}(\alpha,\alpha') - 2\pi i\delta(E(\alpha') - E(\alpha))\, N_{\alpha'}^{\frac{1}{2}} N_{\alpha}^{\frac{1}{2}} \\ \Sigma_\delta \langle\alpha'|\{V - VR(E(\alpha) + i0)V\}_\delta|\alpha\rangle, \qquad (4.17)$$

where $N_{\alpha'}$ and N_α are defined in analogy with (3.5); $E(\alpha)$ is the difference in energy between the physical state $|\alpha\rangle$ and the physical vacuum $|0\rangle$; R is the resolvent and Σ_δ extends over diagrams δ which have the following properties; they have no ground state components, they are not entirely composed of one-particle components, nor is any of the smaller diagrams obtained by erasing in some δ all what is on the left or on the right of an intermediate state.

Consider the diagram of fig. 11, contributing to

$$\langle(\boldsymbol{p}' - \boldsymbol{k}_s)_{r'};\, s\lambda\,|S|\,\boldsymbol{p}_r;\{0\}\rangle,$$

where the action of an external field W is indicated by the dot on the electron line.

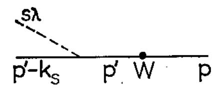

Fig. 11. Bremsstrahlung with the emission of one soft photon.

As $\omega_s \ll m$ we can calculate the diagram in the Bloch-Nordsieck approximation,

$$\langle(\boldsymbol{p} - \boldsymbol{k}_s)_{r'};\, s\lambda\,|S_{(11)}|\,\boldsymbol{p}_r;\,\{0\}\rangle = -\,2\pi i\delta(E(\boldsymbol{p}' - \boldsymbol{k}_s) + \omega_s - E(\boldsymbol{p})) \\ N_{\boldsymbol{p}}^{\frac{1}{2}} N_{\boldsymbol{p}'}^{\frac{1}{2}} N_{Rs}^{\frac{1}{2}} W(\boldsymbol{p}', r'; \boldsymbol{p}, r).\, i(\boldsymbol{\mu}', \boldsymbol{a}_{s\lambda})/(\omega_s - (\boldsymbol{\mu}', \boldsymbol{k}_s)) = A N_{Rs}, \qquad (4.18)$$

where $\boldsymbol{\mu}' = \boldsymbol{p}'/E(\boldsymbol{p}')$.

When we correct the photon line in fig. 11 to second order, we have to deal with the ten diagrams of fig. 12.
With the aid of the function $f_R(\omega_s, l)$ expanded as in (4.12) we find for their total contribution

$$\langle(\boldsymbol{p}' - \boldsymbol{k}_s)_{r'};\, s\lambda\,|S_{(12)}\,|\boldsymbol{p}_r;\,\{0\}\rangle = A N_{Rs}^{\frac{1}{2}}\,[-\tfrac{1}{8}e^2\omega_s^{-1}\,\Sigma_i\, c_i M_i + \\ +\, e^2(1/3\pi)\,\Sigma_i\, c_i \ln M_i/M_0 + \mathrm{O}(e^2\omega_s/m)], \qquad (4.19)$$

*) See Frazer and Van Hove [11]) (4.20).

where A is the quantity defined in (4.18). (4.18) and (4.19) together give us in second order in e

$$\langle(\boldsymbol{p}' - \boldsymbol{k}_s)_{r'}; s\lambda\,|S_{(11)+(12)}|\,\boldsymbol{p}_r;\{0\}\rangle = AN_{Rs}{}^{(2)\frac{1}{2}}[1 - \tfrac{1}{8}e^2\omega_s{}^{-1}\textstyle\sum_i c_i M_i + $$
$$+ e^2(1/3\pi)\textstyle\sum_i c_i \ln M_i/M_0 + \mathrm{O}(e^2\omega_s/m)] =$$
$$= A[1 + e^2(1/3\pi)\textstyle\sum_i c_i \ln M_i/M_0 + \mathrm{O}(e^2\omega_s/m)], \quad (4.20)$$

where we used (4.14).

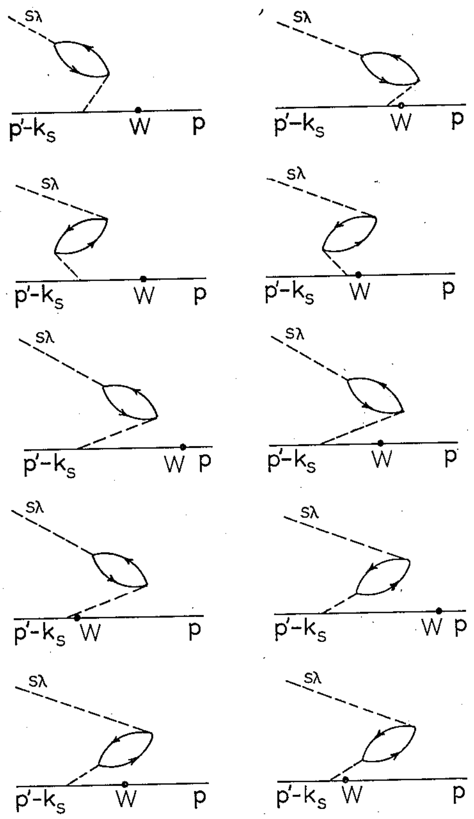

Fig. 12. Second order corrections to fig. 11 in the photon line.

According to renormalization theory the only effect of the corrections in fig. 12 for $\omega_s \to 0$ is to renormalize the charge. In this way we find the renormalized charge e' in second order *)

$$e' = e(1 + e^2(1/3\pi)\textstyle\sum_i c_i \ln M_i/M_0). \quad (4.21)$$

This result agrees with the covariant treatment of Pauli and Villars [10]. In view of (4.14) and (4.21) the assertion by Frazer and Van Hove [11] that $N_{photon} = Z_3$, where Z_3 is the Z-constant of the photon in Dyson's

*) Note that there is no need to use the additional condition (4.15) in deriving (4.21).

notation [15]) (and therefore $Z_3^{\frac{1}{2}}$ the charge renormalization) is hereby shown to be incorrect. The argument given in their paper fails because it disregards the quadratic divergence in the photon self-energy and the need to apply the regularization prescription.

Returning to the problem discussed in section 3 we are now able to show that the diagrams of fig. 8 and fig. 9 only give in (3.9) corrections of relative order $O(e^2\bar{\omega}/m)$, under the condition that the renormalized and unrenormalized charges are put equal. In second order this amounts to putting

$$\textstyle\sum_i c_i \ln M_i/M_0 = 0. \tag{4.22}$$

Indeed, when calculating the contribution C of fig. 3 + fig. 8 to the matrix element $\langle(\boldsymbol{p}-\boldsymbol{k}_s)_r;\, s\lambda|\{\sum_{j=1}^{\infty}(-D^0(E(\boldsymbol{p}))V)^j{}_{n\cdot i}\}|\,\boldsymbol{p}_r;\{0\}\rangle$ (see (3.4)), we find for $\omega_s \ll m$ by making extensive use of the function $f_R(\omega_s, l)$,

$$C = [-2^{-\frac{1}{2}}i(\boldsymbol{\mu}, \boldsymbol{a}_{s\lambda})/(\omega_s - (\boldsymbol{\mu}, \boldsymbol{k}_s))][1 + e^2[\tfrac{1}{8}\omega_s^{-1}\textstyle\sum_i c_i M_i + \\ + (1/3\pi)\textstyle\sum_i c_i \ln M_i/M_0 + O(\omega_s/m)]]. \tag{4.23}$$

In this calculation the terms of order ω_s/m in the electron recoil are already neglected. When applying (4.15) and putting $e' = e$ (i.e. applying (4.22)) we find for C

$$C = [-2^{-\frac{1}{2}}i(\boldsymbol{\mu}, \boldsymbol{a}_{s\lambda})/(\omega_s - (\boldsymbol{\mu}, \boldsymbol{k}_s))][1 + O(e^2\omega_s/m]. \tag{4.24}$$

The diagrams of fig. 9 are treated in a somewhat different way. One readily shows that under the conditions (4.15) and (4.22) the sum over $\boldsymbol{p}'$ and $s\lambda$ of the absolute squared contribution of fig. 9*ab* is of order $e^2\bar{\omega}/m$. The calculation is again based on extensive consideration of the function $f_R(\omega_s, l)$. As higher order corrections in the photon lines of fig. 3 can be treated in a similar way *), we can consider the proof of (3.9) to be complete.

Acknowledgements. The author is greatly indebted to Professor L. Van Hove, who suggested the present investigation, for his most valuable advice and criticism throughout this work. The author is also very grateful to Dr. Th. W. Ruijgrok for many fruitful discussions.

REFERENCES

1) Bloch, F., Nordsieck, A., Phys. Rev. **52** (1937) 54.
2) Jauch, J. M., Rohrlich, F., Helv. Phys. Acta **27** (1954) 613; The theory of photons and electrons. Addison-Wesley Publ. Comp., Inc. pp. 390–405.
3) Lomon, E. L., Nucl. Phys. **1** (1956) 101.
4) Nakanishi, N., Progr. Theor. Phys. **19** (1958) 159.
5) Yennie, D. R., Suura, H., Phys. Rev. **105** (1957) 1378.

---

*) For a treatment of regularization to higher order see Bogoliubov and Shirkov [16]), pp. 364 and foll.

6) Thirring, W., Phil. Mag. **41** (1950) 1193.
7) Brown, L. M., Feynman, R. P., Phys. Rev. **85** (1952) 231.
8) Van Hove, L., Physica **21** (1955) 901; **22** (1956) 343.
9) Hugenholtz, N. M., Physica **23** (1957) 481.
10) Pauli, W., Villars, F., Rev. Mod. Phys. **21** (1949) 434.
11) Frazer, W. R., Van Hove, L., Physica **24** (1958) 137.
12) Schweber, S., Bethe, H. A., De Hoffmann, F., Mesons and Fields. Row, Peterson and Comp.
13) Gupta, S. N., Proc. Phys. Soc. A **66** (1953) 137.
14) Ward, J. C., Phys. Rev. **78** (1950) 182.
15) Dyson, F. J., Phys. Rev. **75** (1949) 1736.
16) Bogoliubov, N. N., Shirkov, D. V., Introduction to the theory of quantized fields. Interscience Publ. Inc.

Chapter II

BREMSSTRAHLUNG AND COMPTON SCATTERING

Synopsis

The infrared aspects of quantum electrodynamics are discussed by treating two examples of scattering processes, bremsstrahlung and Compton scattering. As in the previous paper one uses a non-covariant diagram technique which gives very clear insight in the cancelling of infrared divergences between real and virtual photons. The treatment of Compton scattering shows the necessity of reformulating a theorem of Thirring on the validity of the Thomson scattering formula at very low energies.

1. *Introduction.* The aim of the present paper is to discuss the infrared divergences involved in the S-matrix elements for scattering processes in quantum electrodynamics. The method to be employed is essentially non-covariant and relies on the results of the previous paper [1]), to be referred hereafter as I. For concreteness we treat two examples of scattering processes, *bremsstrahlung* and *Compton scattering*, with all accompanying infrared effects. The main difference between our discussion and the covariant treatment of Jauch and Rohrlich [2]) lies in our extensive use of the non-covariant diagram technique already employed in I. This technique allows a simple and clear-cut separation of all effects of importance in the infrared region; it thereby provides what we believe to be a more convincing and transparant treatment. The problem of Compton scattering in the non-relativistic limit, already mentioned in I because of our objection to the theorem of Thirring [3]), is readily solved within the framework of our analysis.

The three following sections are devoted to the discussion of *bremsstrahlung*. The external field acting on the electron is considered to be weak and we treat it in first Born approximation. In section 3 we introduce a new concept of 'basic diagram' which turns out to be very useful for splitting off infrared divergent effects. In section 4 all infrared divergences are eliminated by redefining the transition probability for *bremsstrahlung* so as to include all processes in which additional unobservably weak radiation is emitted. Section 5 is devoted to the study of low energy Compton scattering in connection with the theorem of Thirring [3]). This theorem can only be made valid through a reformulation taking soft radiation effects properly into account.

2. *The electron in a weak external field. 'Restricted' calculation of S-matrix elements.* The study of the infrared divergences in quantum electrodynamics is started in the present section by discussing the process of bremsstrahlung in the case of a small perturbation acting on the electron. The same example was treated previously by Bloch and Nordsieck [4]), but it is our contention that their treatment is not faultless and certainly incomplete.

The hamiltonian $H = H_0 + V$ (see I. 3.2) is extended with a small perturbation W

$$W = \Sigma_{pp'rr'} [b_{r'}^*(\mathbf{p}')b_r(\mathbf{p})\, w_1(\mathbf{p}',r';\mathbf{p},r) + b_{r'}^*(\mathbf{p}')\, d_r^*(\mathbf{p})\, w_2(\mathbf{p}',r';\mathbf{p},r) + \\ + d_{r'}(\mathbf{p}')\, b_r(\mathbf{p})\, w_3(\mathbf{p}',r';\mathbf{p},r) + d_{r'}(\mathbf{p}')d_r^*(\mathbf{p})w_4(\mathbf{p}',r';\mathbf{p},r)] \quad (2.1)$$

This perturbation will be treated in first Born approximation. We want to study transitions caused by W between the one-electron state $|\mathbf{p}_r; \{0\})$ and states $|\mathbf{p}_{r'}; \{n_{s\lambda}\})$ where $\Sigma_{s\lambda} n_{s\lambda}\omega_s \leq \Delta\varepsilon$, $\Delta\varepsilon \leq \bar{\omega}$ being so small that the individual photons in the final state will not be observed. The energy loss of the electron is then also $\leq \Delta\varepsilon$. The transitions are studied with the S-matrix in the form (I. 4.17)

$$\langle \mathbf{p}'_{r'}; \{n_{s\lambda}\} |S| \mathbf{p}_r; \{0\}\rangle = \delta_{pp'}\delta_{rr'}\delta_{\{0\},\{n_{s\lambda}\}} - 2\pi i \delta(E(\mathbf{p}') + \Sigma_{s\lambda} n_{s\lambda}\omega_s - E(\mathbf{p})) \\ N_p^{\frac{1}{2}} N^{\frac{1}{2}}_{p',\{n_{s\lambda}\}} \Sigma_\delta \langle \mathbf{p}'_{r'}; \{n_{s\lambda}\} |\{V' - V'R'(E(\mathbf{p}) + i0)\, V'\}_\delta| \mathbf{p}_r; \{0\}\rangle \quad (2.2)$$

where

$$N_{p',\{n_{s\lambda}\}} = N_{p'} N_{\{n_{s\lambda}\}};\ V' = V + W$$

and

$$R'(z) = (H_0 + V + W - z)^{-1} = \\ = D^0(z) - D^0(z)\, V'D^0(z) + D^0(z)\, V'D^0(z) V'D^0(z) - \ldots\ldots \quad (2.3)$$

As W is to be treated in first Born approximation we only consider diagrams δ with one W-interaction (a W-interaction is indicated with a dot).

In the present section we calculate the matrix elements (2.2) only partially: we want to restrict ourselves to diagrams δ with the following two properties

1. Each photon line in δ represents a photon with energy $\leq \bar{\omega}$ (photons satisfying this condition are represented by dotted lines).

2. The W-interaction in δ produces no positron emission or absorption and consequently originates from the following part of W

$$W' = \Sigma_{p'pr'r}\, b_{r'}^*(\mathbf{p}')\, b_r(\mathbf{p})\, w_1(\mathbf{p}',r';\mathbf{p},r). \quad (2.4)$$

$w_1(\boldsymbol{p}', r'; \boldsymbol{p}, r)$ can be considered as the fourier transform of the potential $W(\boldsymbol{r})$ acting on the electron

$$w_1(\boldsymbol{p}', r'; \boldsymbol{p}, r) = \Omega^{-1} \int \mathrm{d}_3\boldsymbol{r}\; u_{r'}^*(\boldsymbol{p}')\; W(\boldsymbol{r})\; u_r(\boldsymbol{p})\; e^{-i((\boldsymbol{p}'-\boldsymbol{p}),\boldsymbol{r})} \tag{2.5}$$

where u and u^* are the electron spinors.

The reason of this restricted calculation is that it is essentially the same as the calculation of Bloch and Nordsieck (In the following section we will take into account all diagrams δ). We will find the well known result that each matrix element (2.2) and consequently the corresponding transition probability are zero. This will turn out to be true for the restricted calculation (this section) as well as for the complete calculation (following section).

If we restrict ourselves to photon energies $\leq \bar{\omega}$, we can write in accordance with (I. 2.16b) and (I. 3.9)

$$N_p \simeq \overline{N}_p = \exp[-\tfrac{1}{2}\Sigma^{\bar{\omega}}_{s\lambda}\, \sigma^2_{ps\lambda}] \tag{2.6}$$

where we made a small change in notation $\overline{N}_\mu \to \overline{N}_p$ and $\sigma_{\mu s\lambda} \to \sigma_{ps\lambda}$. In accordance with (I. 4.14) and (I. 4.15) we can write

$$N_{\{n_{s\lambda}\}} = \Pi_{s\lambda}\, N_s^{n_{s\lambda}} \simeq 1. \tag{2.7}$$

In writing (2.6) and (2.7) we make errors of relative order $e^2\bar{\omega}/m$. The exponential (2.6) tends to zero in the limit of large volume Ω, because of the logarithmic divergence of the sum $\Sigma^{\bar{\omega}}_{s\lambda}\, \sigma^2_{ps\lambda}$ at low frequencies. This is the main reason why the S-matrix elements (2.2) are all zero. If the photon had a finite rest mass, the exponential would not vanish, because of non vanishing energy denominators in the σ's in the low frequency region.

Let us calculate first the matrix element $\langle \boldsymbol{p}'_{r'}; \{0\}\, |S|\, \boldsymbol{p}_r; \{0\}\rangle$ where no photon is present neither in the initial nor in the final state. The lowest order contribution to it comes from the diagram of fig. 1 and is found to be

$$\{\langle \boldsymbol{p}'_{r'}; \{0\}\, |S|\, \boldsymbol{p}_r; \{0\}\rangle\}_0 =$$
$$= -\,2\pi i\delta(E(\boldsymbol{p}') - E(\boldsymbol{p}))\; w_1(\boldsymbol{p}', r'; \boldsymbol{p}, r)\; \exp[-\tfrac{1}{4}\, \Sigma^{\bar{\omega}}_{s\lambda}(\sigma^2_{ps\lambda} + \sigma^2_{p's\lambda})]. \tag{2.8}$$

Fig. 1. Lowest order diagram contributing to $\langle \boldsymbol{p}'_{r'}; \{0\}|S|\boldsymbol{p}_r; \{0\}\rangle$.

When calculating radiative corrections to (2.8) with the two restrictions mentioned above, it is found in a way quite similar to the method followed in (I. 3) and (I. 4) that one can forget all diagrams in which electron-positron pairs are created and absorbed. Furthermore one can forget all corrections coming from virtual photons which are emitted and absorbed on one and the same side of the W'-point. By leaving out all these diagrams we make errors of relative order $e^2\bar{\omega}/m$. So we have only to deal with diagrams in which the virtual photons overlap the W'-point (see for instance the diagram of fig. 2).

In these diagrams we can neglect the electron's recoil due to the emission and absorption of the virtual photons, in complete analogy with (I. 3).

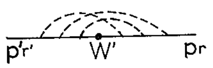

Fig. 2. Example of a radiative correction to the diagram of fig. 1. The virtual photons overlap the W'-point.

It is not allowed to restrict oneself to radiative corrections up to a given order, because of the fact that additional soft photon lines give rise to additional infrared divergent integrals. So we want to sum over all possible soft photon corrections of all orders. This can be done exactly if we take as a last approximation that in each diagram the interaction W' gives rise to a constant factor $w_1(\boldsymbol{p}', r'; \boldsymbol{p}, r)$. We then find after some combinatorics

$$\langle \boldsymbol{p}'_{r'}; \{0\} | S | \boldsymbol{p}_r; \{0\} \rangle = \{\langle \boldsymbol{p}'_{r'}; \{0\} | S | \boldsymbol{p}_r; \{0\}\rangle\}_0 \textstyle\sum_{m=0}^{\infty} \{\frac{1}{2} \sum_{s\lambda}^{\varpi} \sigma_{p's\lambda} \sigma_{ps\lambda}\}^m / m! =$$
$$= -2\pi i \delta(E(\boldsymbol{p}') - E(\boldsymbol{p}))\, w_1(\boldsymbol{p}', r'; \boldsymbol{p}, r) \exp[-\tfrac{1}{4} \textstyle\sum_{s\lambda}^{\varpi} (\sigma_{p's\lambda} - \sigma_{ps\lambda})^2]. \quad (2.9)$$

The error made in (2.9) due to the fact that we took w_1 as a constant factor can at most be of relative order $e^2\bar{\omega}/m$. This is based on the observation that (see (2.5))

$$w_1(\boldsymbol{p}' - \boldsymbol{k}_s, r'; \boldsymbol{p} - \boldsymbol{k}_s, r) = w_1(\boldsymbol{p}', r'; \boldsymbol{p}, r)(1 + O(\omega_s / E(\boldsymbol{p}))). \quad (2.10)$$

The expression (2.9) vanishes due to the infrared behaviour of the exponential.

We now want to calculate the S-matrix element $\langle \boldsymbol{p}''_{r'}; \{n_{s\lambda}\} | S | \boldsymbol{p}_r; \{0\}\rangle$ for a final state with $\{n_{s\lambda}\} \neq \{0\}$. We choose the final electron momentum $\boldsymbol{p}''$ to have the same direction as $\boldsymbol{p}'$ in (2.9). This choice is justified by the fact that the processes $\boldsymbol{p}_r; \{0\} \rightarrow \boldsymbol{p}'_{r'}; \{0\}$ and $\boldsymbol{p}_r; \{0\} \rightarrow \boldsymbol{p}_r''; \{n_{s\lambda}\}$ are physically indistinguishable. Fig. 3 gives an example of a diagram contributing to $\langle \boldsymbol{p}''_{r'}; \{n_{s\lambda}\} | S | \boldsymbol{p}_r; \{0\}\rangle$. One has to sum over all diagrams of this kind in which the number of virtual soft photon lines varies and in which all vertices are permuted in all different ways.

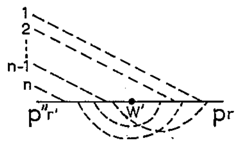

Fig. 3. Example of a diagram contributing to $\langle \boldsymbol{p}''_{r'}; \{n_{s\lambda}\} | S | \boldsymbol{p}_r; \{0\}\rangle$ in which $n = \sum_{s\lambda} n_{s\lambda}$ is the number of real soft photons emitted.

Again one can verify that diagrams with pairs are irrelevant while all virtual photons have to overlap the W'-point.

As follows from energy conservation we have the following relation between the final momenta $\boldsymbol{p}''$ and $\boldsymbol{p}'$,

$$\boldsymbol{p}'' = \boldsymbol{p}'(1 + O(\Sigma_{s\lambda}\, n_{s\lambda}\omega_s/(E-m))),$$

where $E - m$ is the kinetic energy of the electron. We want to neglect the difference between $\boldsymbol{p}''$ and $\boldsymbol{p}'$. Furthermore we want again to take w_1 as a constant factor in each diagram. However we observe from (2.5) that w_1 is a function of $\Delta\boldsymbol{p} = \boldsymbol{p}' - \boldsymbol{p}$. When w_1 is taken as a constant factor, the errors we make are $O(e^2\bar{\omega}/m)$ and $O(e^2\Delta\varepsilon/\mu\,|\Delta\boldsymbol{p}|)$. If $|\Delta\boldsymbol{p}/\boldsymbol{p}| = O(1)$, the last error is $O(e^2\Delta\varepsilon/(E-m))$. If we neglect the difference between $\boldsymbol{p}''$ and $\boldsymbol{p}'$ we find that it is again possible to sum up exactly all contributing diagrams, the result of this combinatorial problem being

$$\begin{aligned}\langle \boldsymbol{p}'_{r'};\{n_{s\lambda}\}|S|\,\boldsymbol{p}_r;\{0\}\rangle &= \langle \boldsymbol{p}'_{r'};\{0\}|S|\,\boldsymbol{p}_r;\{0\}\rangle\, \Pi_{s\lambda}\,(2^{-\frac{1}{2}}i(\sigma_{p's\lambda}-\sigma_{ps\lambda}))^{n_{s\lambda}}/(n_{s\lambda}!)^{\frac{1}{2}} = \\ &= -\,2\pi i\;\delta(E(\boldsymbol{p}')-E(\boldsymbol{p}))\;w_1(\boldsymbol{p}',r';\boldsymbol{p},r)\;\exp[-\tfrac{1}{4}\,\Sigma^{\varpi}_{s\lambda}\,(\sigma_{p's\lambda}-\sigma_{ps\lambda})^2] \\ &\qquad \Pi_{s\lambda}(2^{-\frac{1}{2}}\,i(\sigma_{p's\lambda}-\sigma_{ps\lambda}))^{n_{s\lambda}}/(n_{s\lambda}!)^{\frac{1}{2}}. \qquad (2.11)\end{aligned}$$

The expression (2.11) vanishes just like (2.9) due to the infrared behaviour of the exponential.

3. *The electron in a weak external field. Complete calculation of S-matrix elements.* In this section we want to extend the calculations of the preceding section. We want to calculate matrix elements

$$\langle \boldsymbol{p}'_{r'};\{0\}\,|S|\,\boldsymbol{p}_r;\{0\}\rangle \quad\text{and}\quad \langle \boldsymbol{p}''_{r'};\{n_{s\lambda}\}\,|S|\,\boldsymbol{p}_r;\{0\}\rangle,$$

taking now into account all diagrams δ with one W-interaction, without the two restrictions mentioned in section 2. However, in order to avoid ultraviolet divergences we introduce a high energy cut off $K \gg m$. This will be the only restriction from now on.

As before dotted lines represent soft photons, i.e. photons of frequency $< \bar{\omega}$. By a shaded area as in fig. 4 we represent a connected part of a diagram where each intermediate state (if any) has an energy denominator $> \bar{\omega}$, and from (in) which no electron, positron or photon lines leave (enter) except the two external electron lines drawn in the figure.

Fig. 4. Part of a diagram where each intermediate state in the shaded area has an energy denominator $> \bar{\omega}$.

In such a part the external electron path can be straight (no pairs in intermediate states except for closed loops) or not. Consequently if a W-interaction is involved in such a part, we have not only to deal with interactions of the form (2.4), but there may occur W-terms with positron operators (see

(2.1)). A shaded area containing a W-interaction will be called a basic part of a diagram. By basic diagram we mean a S-matrix diagram without energy denominator $< \bar{\omega}$, consisting of a basic part and an ingoing and outgoing electron line.

Fig. 5. Basic diagram contributing to $\langle \boldsymbol{p}'_{r'}; \{0\}|S|\boldsymbol{p}_r; \{0\}\rangle$.

Let fig. 5 represent all basic diagrams contributing to $\langle \boldsymbol{p}'_{r'}; \{0\}\,|S|\,\boldsymbol{p}_r; \{0\}\rangle$ (the diagram of fig. 1 is one of them). Let the total contribution of their basic parts to the S-matrix element be the factor $B(\boldsymbol{p}', r'; \boldsymbol{p}, r)$. Then the contribution of fig. 5 to $\langle \boldsymbol{p}'_{r'}; \{0\}\,|S|\,\boldsymbol{p}_r; \{0\}\rangle$ is found to be

$$\{\langle \boldsymbol{p}'_{r'}; \{0\}|S|\,\boldsymbol{p}_r; \{0\}\rangle\}_{basic} = -2\pi i\, \delta(E(\boldsymbol{p}')-E(\boldsymbol{p}))\, B(\boldsymbol{p}',r'; \boldsymbol{p}, r)\, N_p^{\frac{1}{2}} N_{p'}^{\frac{1}{2}}. \quad (3.1)$$

We now claim that we find the complete matrix element

$$\langle \boldsymbol{p}'_{r'}; \{0\}\,|S|\,\boldsymbol{p}_r; \{0\}\rangle$$

by taking into account all radiative corrections to basic diagrams fig. 5. If such an additional correction only gives rise to another basic diagram, the contribution is already included in (3.1). So we only have to consider radiative corrections which do not give rise to other basic diagrams. We first consider all second order corrections of this kind. They are represented by the diagrams of fig. 6*a*, 6*b* and 6*c* in which the additional virtual photon is naturally soft.

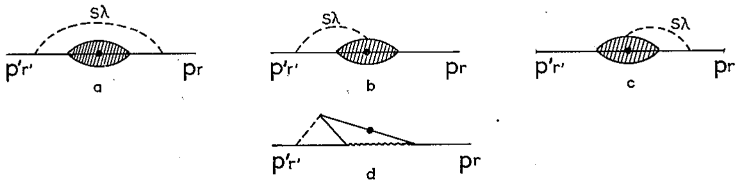

Fig. 6. Second order radiative corrections to fig. 5.

In the case fig. 6*a* the soft photon $s\lambda$ gives rise to two energy denominators $< \bar{\omega}$, which gives an infrared divergent integral over ω_s. In the case fig. 6*bc* the additional soft photon gives rise to only one energy denominator $< \bar{\omega}$, because of the fact that the soft photon is attached at one end to the basic part (Whenever, like in fig. 6*b* and 6*c* a soft photon is attached to a basic part, we count as basic parts also such 'deformed basic parts' in which the soft photon is attached to a vertex where a pair is absorbed or created. An example is given in fig. 6*d* where the wavy line represents a photon of frequency $\geq \bar{\omega}$). In spite of the occurrence of one small energy denominator the integral over ω_s converges in the case fig. 6*bc*. The contribution as compared with that of fig. 5 is of relative order $e^2 f(\bar{\omega}/m)$ in which $\lim_{\varpi \to 0} f(\bar{\omega}/m) = 0$, and will therefore be neglected.

We now look for higher order radiative corrections to fig. 5 (as a matter of course limiting ourselves to those which don't give rise to diagrams of the type fig. 5 and fig. 6 again). In this connection we first restrict ourselves to basic diagrams with only additional virtual soft photon lines. This is the only class of diagrams involved in the considerations of Jauch and Rohrlich [2]) in their treatment of infrared difficulties. (As shown later there are more diagrams to be considered but they will turn out to be irrelevant). We can easily see that diagrams which are constructed from basic diagrams by adding virtual soft photon lines which all overlap the basic part give rise to very important infrared contributions. This case is quite analogous to fig. 2. Here also the main contributions come from diagrams where the electron path outside the basic part is straight. See for instance fig. 7 where we drew the diagrams with two soft photons. Again in analogy with section 2 we can forget all corrections coming from virtual soft photons which are emitted and absorbed on one and the same side of the basic part.

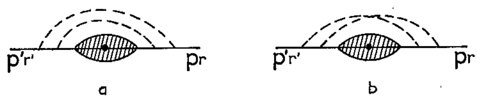

Fig. 7. Fourth order radiative corrections to fig. 5 with only overlapping virtual soft photon lines.

If at least one of the additional soft photon lines is attached to the basic part we can neglect its contribution. See for instance fig. 8 where we drew all fourth order corrections to fig. 5 in which one of the photons is attached to the basic part and where the electron path outside the basic part is straight. We easily find that the contribution of the diagrams of fig. 8 as compared with that of fig. 6*a* is of relative order $e^2 f(\bar{\omega}/m)$ (see above), and can therefore be neglected. The reason is that we have for fig. 8 one small energy denominator less than in the case of fig. 7.

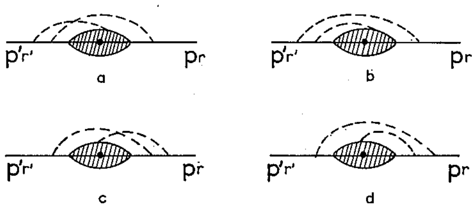

Fig. 8. Fourth order radiative corrections to fig. 5. One of the two virtual soft photons is attached to the basic part.

These considerations can easily be extended to any order, the result being that only virtual soft photon lines overlapping the basic part are relevant, the electron path outside the basic part being straight.

Until now we restricted ourselves to the simple insertion of soft photon lines in fig. 5. But it is possible to construct radiative corrections to fig. 5 with shaded areas outside the basic part. Such corrections are missed in the treatment of Jauch and Rohrlich [2]). First of all we deal with diagrams of the kind fig. 9 in which the shaded areas are in the electron path outside the basic part.

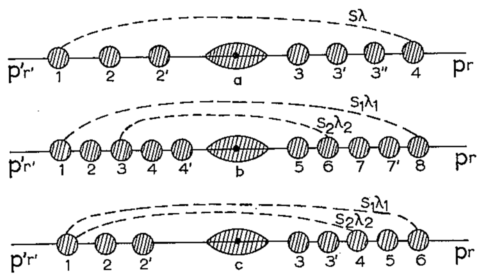

Fig. 9. Higher order radiative corrections to fig. 5 with shaded areas outside the basic part in the electron path.

Consider fig. 9*a*. In the limit $\omega_s \to 0$ the shaded area 1 will compensate the areas 2, 2′, ... due to the Ward identity. The areas 2, 2′, ... simply give rise in this limit to a factor $\tilde{N}_{p'} - 1$ (where $\tilde{N}_{p'}$ equals $N_{p'}$ except for infrared contributions), which compensates with a factor coming from the area 1 in the vertex. Also area 4 and areas 3, 3′, 3″, ... will compensate in the limit $\omega_s \to 0$. We may therefore neglect the diagram of fig. 9*a* as compared with fig. 6*a*. The error will be of relative order $e^2\bar{\omega}/m$.

Consider fig. 9*b*. Quite analogous to the case fig. 9*a* the following pairs of areas will compensate in the limit $\omega_{s_1}, \omega_{s_2} \to 0$; 1 with 2, 2′, ...; 3 with 4, 4′, ...; 6 with 5, 5′, ...; 8 with 7, 7′, ...

Consider fig. 9*c*. The areas 3, 3′, ... and 4; 5, 5′, ... and 6 will compensate, but the areas 1 and 2, 2′, ... will not. As we saw already the areas 2, 2′, ... give rise to a non infrared divergent factor $\tilde{N}_{p'} - 1$ in the limit $\omega_{s_1}, \omega_{s_2} \to 0$. The area 1 is such that one has one small energy denominator less than in the case fig. 7*a*. For that reason diagrams with shaded areas in (from) which more than one soft photon enters (leaves) can be neglected. All these arguments can be extended to higher order diagrams leading to the conclusion that radiative corrections to basic diagrams with shaded areas in the electron path outside the basic part can be neglected.

Secondly we have to deal with diagrams of the kind fig. 10 in which the shaded areas are in the virtual soft photon lines. Using similar arguments as in (I. 4) we can prove that the diagrams of fig. 10*a* and 10*b* and similar diagrams can be neglected, the error being at most of relative order $e^2\bar{\omega}/m$.

The conclusion of the whole diagram analysis is the following: In order to calculate $\langle \boldsymbol{p}'_{r'}; \{0\} | S | \boldsymbol{p}_r; \{0\} \rangle$ we have only to deal with diagrams constructed from basic diagrams by adding virtual soft photon lines which overlap the basic part. If in summing up all those diagrams we take the

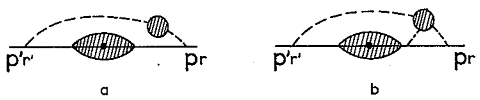

Fig. 10. Higher order radiative corrections to fig. 5 with shaded areas outside the basic part in the virtual soft photon lines.

basic part as a constant factor, we can make at most errors of relative order $e^2 f(\bar{\omega}/m)$ with $\lim_{\varpi \to 0} f(\bar{\omega}/m) = 0$. We find

$$\langle \boldsymbol{p}'_{r'}; \{0\} |S| \boldsymbol{p}_r; \{0\}\rangle = - 2\pi i\, \delta(E(\boldsymbol{p}') - E(\boldsymbol{p}))\, B(\boldsymbol{p}', r'; \boldsymbol{p}, r)$$
$$N_p^{\frac{1}{2}} N_{p'}^{\frac{1}{2}} \sum_{m=0}^{\infty} \{\tfrac{1}{2} \sum_{s\lambda}^{\varpi} \sigma_{p's\lambda}\, \sigma_{ps\lambda}\}^m / m! \qquad (3.2)$$

where B has the same meaning as in (3.1).

By making a similar diagram analysis with diagrams contributing to $N_p = (1 + ((\partial/\partial l)\, G_p(l))_{l=E(\boldsymbol{p})})^{-1}$ one can prove

$$N_p \simeq \tilde{N}_p \exp[- \tfrac{1}{2} \sum_{s\lambda}^{\varpi} \sigma^2_{ps\lambda}] \qquad (3.3)$$

where, as before, $\tilde{N}_p$ is defined in the same way as N_p except that all photons are restricted to the frequency range $\omega > \bar{\omega}$. The error in writing (3.3) depends on $\bar{\omega}$ and vanishes for $\bar{\omega} \to 0$. With the aid of (3.3) we write for the complete matrix element

$$\langle \boldsymbol{p}'_{r'}; \{0\} |S| \boldsymbol{p}_r; \{0\}\rangle = - 2\pi i\, \delta(E(\boldsymbol{p}') - E(\boldsymbol{p}))\, B(\boldsymbol{p}', r'; \boldsymbol{p}, r)$$
$$\tilde{N}_p^{\frac{1}{2}} \tilde{N}_{p'}^{\frac{1}{2}} \exp[- \tfrac{1}{4} \sum_{s\lambda}^{\varpi} (\sigma_{p's\lambda} - \sigma_{ps\lambda})^2]. \qquad (3.4)$$

This formula can be compared with (2.9) of which it is an extension. Again one easily sees that (3.4) vanishes due to the infrared behaviour of the exponential.

We now want to calculate the complete matrix element

$$\langle \boldsymbol{p}''_{r'}; \{n_{s\lambda}\} |S| \boldsymbol{p}_r; \{0\}\rangle \simeq \langle \boldsymbol{p}'_{r'}; \{n_{s\lambda}\} |S| \boldsymbol{p}_r; \{0\}\rangle \text{ in which } \{n_{s\lambda}\} \neq \{0\}.$$

The diagram analysis which lead to (3.3) and (3.4) is very helpful in this calculation.

First of all we can certainly say that all diagrams of the kind fig. 11 are relevant. Such diagrams are constructed from all relevant diagrams contributing to (3.2), by attaching real soft photon lines to the external lines of the basic diagram. We get a maximal number of small energy denominators in this way. Thus, if we include shaded areas in fig. 11 outside the basic part, we can treat them in a completely analogous way as in figs. 9 en 10. If one of the real soft photon lines in fig. 11 would be attached to the basic part in stead of to an external line, we would have one small energy denominator less. This is enough to neglect the diagram. See for instance the diagram of fig. 12*a*, which will be neglected as compared with fig. 12*b* and 12*c*, because of the fact that for $\omega_s \to 0$ it has no vanishing energy denominator. If one of the virtual soft photon lines in fig. 11 would be attached to the basic part

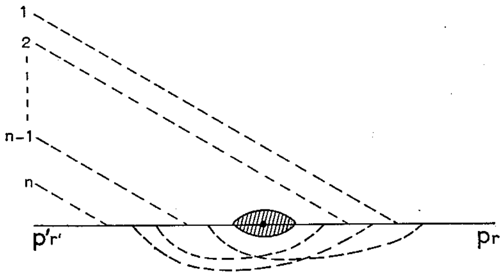

Fig. 11. Example of a diagram contributing to $\langle \boldsymbol{p}'_{r'};\{n_{s\lambda}\}|S|\boldsymbol{p}_r;\{0\}\rangle$, where each drawn soft real or virtual photon is attached to the external lines of the basic diagram.

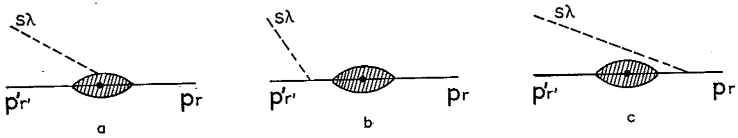

Fig. 12. Basic diagrams with one additional real soft photon.

with one side, in stead of to an external line, we would have also one energy denominator less. Again this is enough to neglect the diagram. See for instance the diagrams of fig. 13*a* and 13*b*. One could have the impression that the diagram of fig. 13*a* is important in the infrared region, because of the fact that for vanishing ω_s the integral over ω_{s_1} converges very badly *). However if we take together the diagrams of fig. 13*a* and 13*b*, the result is a

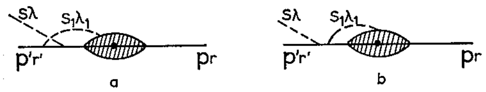

Fig. 13. Basic diagrams with one additional real soft photon. A virtual soft photon is attached to the basic part with one side.

convergent ω_{s_1} integration. So we can simply neglect fig. 13*a* and 13*b* as compared with fig. 12*b*. The result of this discussion is that we only have to sum over all diagrams of the kind fig. 11 in order to get the complete matrix element $\langle \boldsymbol{p}'_{r'};\{0\}|S|\boldsymbol{p}_r;\{0\}\rangle$. Doing this we find the following extension of (2.11)

$$\langle \boldsymbol{p}'_{r'};\{n_{s\lambda}\}|S|\boldsymbol{p}_r;\{0\}\rangle = -2\pi i\,\delta(E(\boldsymbol{p}')-E(\boldsymbol{p}))B(\boldsymbol{p}',r';\boldsymbol{p}\;r)$$
$$\tilde{N}_p^{\frac{1}{2}}\tilde{N}_{p'}^{\frac{1}{2}}\exp[-\tfrac{1}{4}\textstyle\sum_{s\lambda}^{\varpi}(\sigma_{p's\lambda}-\sigma_{ps\lambda})^2]\prod_{s\lambda}(2^{-\frac{1}{2}}i(\sigma_{p's\lambda}-\sigma_{ps\lambda}))^{n_{s\lambda}}/(n_{s\lambda}!)^{\frac{1}{2}}. \quad (3.5)$$

Again the expression (3.5) vanishes due to the behaviour of the exponential.

*) A similar diagram was discussed by Nakanishi [5]), p. 162.

4. *Transition probability of the bremsstrahlung process without observable radiation.* From (3.5) we find the corresponding transition probability per unit time for the process $\boldsymbol{p}_r$; $\{0\} \to \boldsymbol{p}'_{r'}$; $\{n_{s\lambda}\}$ in the form

$$T(\boldsymbol{p}'_{r'}, \{n_{s\lambda}\}; \boldsymbol{p}_r, \{0\}) = 2\pi\, \delta(E(\boldsymbol{p}') - E(\boldsymbol{p}))\, |B(\boldsymbol{p}', r'; \boldsymbol{p}, r)|^2$$
$$\tilde{N}_p \tilde{N}_{p'} \exp[-\tfrac{1}{2}\Sigma_{s\lambda}^{\varpi}(\sigma_{p's\lambda} - \sigma_{ps\lambda})^2]\, \Pi_{s\lambda}\{\tfrac{1}{2}(\sigma_{p's\lambda} - \sigma_{ps\lambda})^2\}^{n_{s\lambda}}/n_{s\lambda}!. \qquad (4.1)$$

Just like (3.5) the expression (4.1) is zero in the limit $\Omega \to \infty$. The reason is clearly the following. Physically it makes little sense to consider (4.1) when none of the emitted photons is observed because of its energy being to low. We therefore want to sum (4.1) over all unobservable sets of photons $\{n_{s\lambda}\}$ so as to get a transition probability which has a more directly observable meaning. This is the well known procedure to interpret in physical terms the infrared divergences of electrodynamics. So we have to sum (4.1) over all sets $\{n_{s\lambda}\}$ with the restriction $\Sigma_{s\lambda}\, n_{s\lambda} \leq \Delta\varepsilon$. We find for this new transition probability the following expression (where the prime in $\Sigma'_{\{n_{s\lambda}\}}$ indicates the restricted summation)

$$\Sigma'_{\{n_{s\lambda}\}}\, T(\boldsymbol{p}'_{r'}, \{n_{s\lambda}\}; \boldsymbol{p}_r, \{0\}) = 2\pi\delta(E(\boldsymbol{p}') - E(\boldsymbol{p}))\, |B(\boldsymbol{p}', r'; \boldsymbol{p}, r)|^2$$
$$\tilde{N}_p \tilde{N}_{p'} \exp[-\tfrac{1}{2}\, \Sigma_{s\lambda}^{\varpi}\, (\sigma_{p's\lambda} - \sigma_{ps\lambda})^2]\, \Sigma'_{\{n_{s\lambda}\}}\, \Pi_{s\lambda}\{\tfrac{1}{2}(\sigma_{p's\lambda} - \sigma_{ps\lambda})^2\}^{n_{s\lambda}}/n_{s\lambda}!. \quad (4.2)$$

Following Jauch and Rohrlich [2]), we can rewrite the restricted summation in (4.2) in a more covenient form if we introduce the identity

$$(2\pi i)^{-1} \textstyle\int_{-\infty}^{+\infty} \mathrm{d}\xi\, \exp[i\xi(1 - \Sigma_{s\lambda}\, n_{s\lambda}\omega_s/\Delta\epsilon)]/(\xi - i\eta) = 1 \text{ if } \Sigma_{s\lambda}\, n_{s\lambda}\omega_s < \Delta\varepsilon$$
$$= 0 \text{ if } \Sigma_{s\lambda}\, n_{s\lambda}\omega_s > \Delta\varepsilon$$

where η is a small positive number.

We write

$$\Sigma'_{\{n_{s\lambda}\}}\, \Pi_{s\lambda}\, \{\tfrac{1}{2}(\sigma_{p's\lambda} - \sigma_{ps\lambda})^2\}^{n_{s\lambda}}/n_{s\lambda}! = \Sigma_{\{n_{s\lambda}\}}\, \Pi_{s\lambda}\, \{\tfrac{1}{2}(\sigma_{p's\lambda} -$$
$$- \sigma_{ps\lambda})^2\}^{n_{s\lambda}}/(n_{s\lambda}!)\cdot \textstyle\int_{-\infty}^{+\infty} \mathrm{d}\xi\, \exp[i\xi(1 - \Sigma_{s\lambda} n_{s\lambda}\omega_s/\Delta\varepsilon)]/(2\pi i(\xi - i\eta)) =$$
$$= \textstyle\int_{-\infty}^{+\infty} \mathrm{d}\xi\, \exp(i\xi)/(2\pi i(\xi - i\eta))\, \exp[\tfrac{1}{2}\, \Sigma_{s\lambda}^{\Delta\varepsilon}(\sigma_{p's\lambda} - \sigma_{ps\lambda})^2\, \exp(-\, i\xi\omega_s/\Delta\varepsilon)]. \; (4.4)$$

We can write in the limit $\Omega \to \infty$

$$\tfrac{1}{2}\Sigma_{s\lambda}(\sigma_{p's\lambda} - \sigma_{ps\lambda})^2 = \alpha C(\boldsymbol{p}', \boldsymbol{p}) \textstyle\int \mathrm{d}\omega/\omega \qquad (4.5)$$

where $\alpha = e^2$ is the fine-structure constant and

$$C(\boldsymbol{p}', \boldsymbol{p}) = (2\pi)^{-2} \int \mathrm{d}\Omega_s\, \Sigma_\lambda \left[\frac{(\boldsymbol{\mu}', \boldsymbol{\varepsilon}_{s\lambda})}{1 - (\boldsymbol{\mu}', \boldsymbol{k}_s)/k_s} - \frac{(\boldsymbol{\mu}, \boldsymbol{\varepsilon}_{s\lambda})}{1 - (\boldsymbol{\mu}, \boldsymbol{k}_s)/k_s}\right]^2, \qquad (4.6)$$

$\mathrm{d}\Omega_s$ being the element of solid angle in the direction of the photon momentum $\boldsymbol{k}_s$; $\boldsymbol{\mu} = \boldsymbol{p}/E(\boldsymbol{p})$; $\boldsymbol{\mu}' = \boldsymbol{p}'/E(\boldsymbol{p}')$ and $k_s = |\boldsymbol{k}_s|$. We thus find

$$\lim_{\Omega\to\infty} \exp[-\tfrac{1}{2}\, \Sigma_{s\lambda}^{\varpi}\, (\sigma_{p's\lambda} - \sigma_{ps\lambda})^2]\, \Sigma'_{\{n_{s\lambda}\}}\, \Pi_{s\lambda}\, \{\tfrac{1}{2}(\sigma_{p's\lambda} - \sigma_{ps\lambda})^2\}^{n_{s\lambda}}/n_{s\lambda}! =$$
$$= \exp[-\, \alpha C(\boldsymbol{p}', \boldsymbol{p})\, \ln \bar{\omega}/\Delta\epsilon] \textstyle\int_{-\infty}^{+\infty} \mathrm{d}\xi\, \exp(i\xi)/(2\pi i(\xi - i\eta))$$
$$\exp[\alpha C(\boldsymbol{p}', \boldsymbol{p}) \textstyle\int_0^1 \mathrm{d}x(\exp(-\, i\xi x) - 1)/x]. \qquad (4.7)$$

The integral over ξ in the right-hand side of (4.7) exists but cannot be found in closed form, the integral over x, however, can. One finds

$$\int_{-\infty}^{+\infty} d\xi \exp(i\xi)/(2\pi i(\xi - i\eta)) \exp[\alpha C(\boldsymbol{p}', \boldsymbol{p}) \int_0^1 dx(\exp(-i\xi x) - 1)/x] =$$
$$= \int_{-\infty}^{+\infty} d\xi \exp(i\xi)/(2\pi i(\xi - i\eta)) \exp[\alpha C(\boldsymbol{p}', \boldsymbol{p}) \{Ci\xi - \ln \gamma\xi - iSi\xi\}] =$$
$$= 1 - (\pi^2/12)\, \alpha^2 C^2(\boldsymbol{p}', \boldsymbol{p}) + \ldots \tag{4.8}$$

where γ is the constant of Euler, and $Ci\xi$ and $Si\xi$ are the integral cosine and sine. (4.8) agrees with the result of Yennie and Suura [6]) p. 1379, eq. (9).

If μ and μ' are $\ll 1$, than $C(\boldsymbol{p}', \boldsymbol{p}) = O((\boldsymbol{\mu}' - \boldsymbol{\mu})^2)$. In that case we find for the right-hand side of (4.8) a result which is practically 1. Only in the case μ, $\mu' \approx 1$ we find deviations from 1, because of the fact that in that case $C(\boldsymbol{p}', \boldsymbol{p})$ becomes very large; the approximation in the right-hand side of (4.8) is then insufficient.

If we rewrite (4.2) with the aid of (4.7) and (4.8) we get

$$\Sigma'_{\{n_{s\lambda}\}} T(\boldsymbol{p}'_{r'}, \{n_{s\lambda}\}; \boldsymbol{p}_r, \{0\}) = 2\pi\delta(E(\boldsymbol{p}') - E(\boldsymbol{p}))\, |B(\boldsymbol{p}', r'; \boldsymbol{p}, r)|^2\, \tilde{N}_p \tilde{N}_{p'}$$
$$\exp[-\alpha C(\boldsymbol{p}', \boldsymbol{p}) \ln \bar{\omega}/\Delta\epsilon](1 - (\pi^2/12)\, \alpha^2 C^2(\boldsymbol{p}', \boldsymbol{p}) + \ldots). \tag{4.9}$$

If we specialize to the case μ, $\mu' \ll 1$, we can forget the last factor in (4.9), and so we get finally

$$\Sigma'_{\{n_{s\lambda}\}} T(\boldsymbol{p}'_{r'}, \{n_{s\lambda}\}; \boldsymbol{p}_r, \{0\}) = 2\pi\delta(E(\boldsymbol{p}') - E(\boldsymbol{p}))\, |B(\boldsymbol{p}', r'; \boldsymbol{p}, r)|^2 \tilde{N}_p \tilde{N}_{p'}$$
$$\exp[-\alpha C(\boldsymbol{p}', \boldsymbol{p}) \ln \bar{\omega}/\Delta\varepsilon]. \tag{4.10}$$

We derived the expression (4.10) under the following conditions e^2, $\bar{\omega}/m$, $e^2\Delta\varepsilon/\mu\, |\Delta\boldsymbol{p}|$, $\mu \ll 1$. It is worth noting that the expression (4.10) could be derived without the restriction $\Sigma_{s\lambda}\, n_{s\lambda}\, \omega_s \leq \Delta\varepsilon$. The same expression would be found if each real soft photon individually had its energy in the interval $(0, \Delta\varepsilon)$. The only effect of the restricted summation is the factor $(1 - (\pi^2/12)\, \alpha^2 C^2(\boldsymbol{p}', \boldsymbol{p}) + \ldots)$ in (4.9), which was not found by Bloch and Nordsieck [4]). In the treatment of Jauch and Rohrlich [2]) the restriction on the real soft photons is taken into account.

In actual practice the function $\tilde{N}_p \tilde{N}_{p'}\, |B(\boldsymbol{p}', r';\, \boldsymbol{p}, r)|^2$ in (4.10) is approximated by all basic parts up to a given order in α. Expressed in terms of renormalized charge and mass it has a finite limit when the ultraviolet cut off tends to infinity. It of course involves the infrared cut off $\bar{\omega}$.

The exponential factor in (4.10) is the effect of all possible soft photon corrections (real and virtual) to infinite order. In this exponential factor, as we saw already, $C(\boldsymbol{p}', \boldsymbol{p}) = O((\boldsymbol{\mu}' - \boldsymbol{\mu})^2)$ in the non-relativistic region μ, $\mu' \ll 1$. Further $\bar{\omega} = fm$ where $0 < f \ll 1$, while the whole $\Delta\epsilon$-dependence of (4.10) is located in the expression $\ln \bar{\omega}/\Delta\varepsilon$.

Assume that C is not too large, $C \lesssim 1$. This holds as long as we are not in the extreme relativistic region. Then, since $\alpha \ll 1$ we can choose $\Delta\epsilon$ such not a good estimate (much too optimistic)

that $fm \gg \Delta\varepsilon \gg fm \exp[-(\alpha C(\boldsymbol{p}', \boldsymbol{p}))^{-1}]$ and we can certainly write

$$\exp[-\alpha C(\boldsymbol{p}', \boldsymbol{p}) \ln \bar{\omega}/\Delta\varepsilon] \simeq 1 - \alpha C(\boldsymbol{p}', \boldsymbol{p}) \ln fm/\Delta\varepsilon \simeq 1. \qquad (4.11)$$

This means that there is a whole $\Delta\varepsilon$-region in which all infrared divergent soft photon corrections (real and virtual) can be neglected. If one considers only second order corrections of this kind one obtains in (4.11) the term of order 1 in α. However, if $\Delta\epsilon$ decreases (the accuracy of the experiment getting better) the approximation (4.11) is getting correspondingly worse. If $\Delta\varepsilon \lesssim fm \exp[-(\alpha C(\boldsymbol{p}' . \boldsymbol{p}))^{-1}]$ one has to take more terms in the expansion of the exponential. The behaviour for $\Delta\varepsilon \to 0$ is clearly singular in α. The transition probability approaches zero whereas its expansion to any finite order in α diverges. The vanishing of the transition probability (4.10) for $\Delta\varepsilon \to 0$ is in agreement with the fact that processes in which the electron is scattered cannot take place without emission of radiation.

5. *Application to Compton scattering in the non-relativistic limit.* In 1950 W. Thirring [3]) established a theorem which can be formulated as follows: the Compton scattering cross section with all radiative corrections reduces in the non-relativistic limit to the second order cross section (i.e. to the Thomson scattering formula). The only effect of the radiative corrections in this limit is to renormalize mass and charge.

As it stands this theorem cannot be strictly correct in view of the fact that in calculating radiative corrections to a certain process one has necessarily to deal with infrared divergent integrals which are not removed by means of a renormalization method of the ultraviolet type. In the case of bremsstrahlung the effect of these infrared divergent integrals was, that each matrix element between states with a finite number of photons vanished, if we took into account all radiative corrections (see (3.5)). We naturally expect the same to be true in the case of Compton scattering. Furthermore we expect in analogy with section 4 that it will be necessary to redefine the transition probability for Compton scattering, taking into account all processes with additional real soft photon production. We will see in this section that it is possible to derive a result very analogous to Thirring's [3]) by including with ordinary (single photon) Compton scattering all multiple Compton processes where the additional real soft photons are of unobservably low energy. The theorem of Thirring [3]) will thus appear to be incorrect inasmuch as it neglects these multiple processes.

We first repeat the arguments leading to the Thirring theorem *).

All possible Feynman diagrams contributing to single photon Compton scattering can be constructed by attaching in all possible ways an ingoing and an outgoing photon line to all electron self-energy diagrams. These two external photon lines can be

*) See Thirring [3]) and Jauch and Rohrlich [7]) p. 246, 247.

attached either to the open electron path or to closed loops. If at least one of the external photon lines is attached to a closed loop, the contribution of such a diagram will vanish if the momentum of that photon approaches zero. Since in the non-relativistic limit the photons have very low momentum we have only to deal with diagrams in which the photon lines are attached to the open electron path. In the case of zero momentum of the external photon lines, every propagation function $S_F(p)$ to which such a line has been attached is replaced by

$$c \Sigma_\mu S_F(p)\, e_\mu \gamma_\mu\, S_F(p) = -ic \Sigma_\mu e_\mu (\partial/\partial p_\mu)\, S_F(p) \tag{5.1}$$

where c is a constant and e_μ the polarization four-vector of the photon. The sum of lowest order Compton scattering and all its radiative corrections in the case that the two external photon momenta are zero is therefore proportional to

$$S_F^{-1}(p)\, \Sigma_{\mu\nu}\, e_\mu{}^{(1)} e_\nu{}^{(2)} [(\partial^2/\partial p_\mu \partial p_\nu)\, S_F'(p)]\, S_F^{-1}(p) \tag{5.2}$$

where $e^{(1)}$ and $e^{(2)}$ are the polarization vectors of the incoming and outgoing photons respectively, and $S_F'(p)$ is the propagation function with all radiative corrections included.

After renormalization of mass one has according to Dyson [8])

$$S_F'(p) = (1 - B)(S_F(p) + \Sigma_f(p)) \tag{5.3}$$

where B is an infinite renormalization constant, and $\Sigma_f(p)$ is the correction to $S_F(p)$ remaining after all renormalization. The conventional argument now says that by choosing the special gauge with $e_0{}^{(1)} = e_0{}^{(2)} = 0$ and specializing to the rest system of the incoming electron ($\boldsymbol{p} = 0$) one finds

$$S_F^{-1}(p)\, [\Sigma_{\mu\nu}\, e_\mu{}^{(1)} e_\nu{}^{(2)} (\partial^2/\partial p_\mu \partial p_\nu)\, \Sigma_f(p)]\, S_F^{-1}(p) = 0. \tag{5.4}$$

Explicit calculations, however, do not confirm this equation because of the appearance of infrared divergent terms in $\Sigma_f(p)$ (see Jauch and Rohrlich [7]) p. 183, eq. (9.26) or p. 463, eq. (A V–28)) which make the separation (5.3) ambiguous. Accepting (5.4), one finds for the remaining part of (5.2)

$$(1 - B)\, S_F^{-1}(p)\, \Sigma_{\mu\nu}\, e_\mu{}^{(1)} e_\nu{}^{(2)} [(\partial^2/\partial p_\mu \partial p_\nu) S_F(p)] S_F^{-1}(p). \tag{5.5}$$

The factor $(1 - B)$ is compensated by the renormalization of the wave functions u and u' of the ingoing and outgoing electron

$$u = (1 - B)^{-\frac{1}{2}} u_R;\; u' = (1 - B)^{-\frac{1}{2}} u'_R \tag{5.6}$$

where u_R and u'_R are the renormalized wave functions. In view of this one finds in stead of (5.5)

$$\begin{aligned} S_F^{-1}(p)\, \Sigma_{\mu\nu}\, e_\mu{}^{(1)} e_\nu{}^{(2)} [(\partial^2/\partial p_\mu \partial p_\nu)\, S_F(p)]\, S_F^{-1}(p) &= \\ = -\Sigma_{\mu\nu}\, [e_\mu{}^{(1)} \gamma_\mu S_F(p)\, e_\nu{}^{(2)} \gamma_\nu + e_\nu{}^{(2)} \gamma_\nu S_F(p) e_\mu{}^{(1)} \gamma_\mu] \end{aligned} \tag{5.7}$$

which is clearly the S-matrix element for Compton scattering to second order. Since we are in the non-relativistic case the corresponding cross section is given by the Thomson formula. The only effect of all radiative corrections was to renormalize the mass. If we consider also all corrections in the external soft photon lines, the effect is an additional charge renormalization.

According to Thirring [3]) as well as to Jauch and Rohrlich [7]) these arguments are sufficient to conclude to the validity of the Thirring theorem. They overlook, however, the occurrence of infrared divergences in radiative corrections and the related emission of infinitely many soft photons in the scattering process.

In order to arrive at a better description of low-energy Compton scattering, we work in analogy with the preceding sections in the non-covariant formalism. Transitions are studied again with the S-matrix in the form (I. 4.17). We want to consider the matrix element $\langle \boldsymbol{p}'_{r'}; s_2\lambda_2 |S| \boldsymbol{p}_r; s_1\lambda_1\rangle$ for Compton scattering, with small but fixed $\boldsymbol{k}_{s_1}$ and $\boldsymbol{k}_{s_2}$ ($\omega_{s_1}, \omega_{s_2} \ll m$). The indices r, r' for the spin of the electron are omitted in the following. The incoming velocity of the electron is denoted by $\boldsymbol{\mu}$. We consider here only the non-relativistic case where $\mu \ll 1$. Let us first calculate the lowest order contribution. There are four second order diagrams (fig. 14). The two diagrams fig. 14a and 14b together give rise to the follownig contribution

$$\{\langle \boldsymbol{p}'; s_2\lambda_2|S|\boldsymbol{p}; s_1\lambda_1\rangle\}_{a+b} =$$
$$= -2\pi i\delta(E(\boldsymbol{p}') + \omega_{s_2} - E(\boldsymbol{p}) - \omega_{s_1})\, \delta_{Kr}(\boldsymbol{p}' + \boldsymbol{k}_{s_2} - \boldsymbol{p} - \boldsymbol{k}_{s_1})$$
$$\tilde{N}_{p'}{}^{\frac{1}{2}}\tilde{N}_{p}{}^{\frac{1}{2}} \exp[-\tfrac{1}{4}\textstyle\sum_{s\lambda}^{\varpi} (\sigma^2{}_{p's\lambda} + \sigma^2{}_{ps\lambda})](\boldsymbol{\mu}, \boldsymbol{a}_{s_1\lambda_1})\, (\boldsymbol{\mu}, \boldsymbol{a}_{s_2\lambda_2})[((\boldsymbol{\mu}, \boldsymbol{k}_{s_1}) - \omega_{s_1})^{-1} -$$
$$- ((\boldsymbol{\mu}, \boldsymbol{k}_{s_2}) - \omega_{s_2})^{-1}]. \quad (5.8)$$

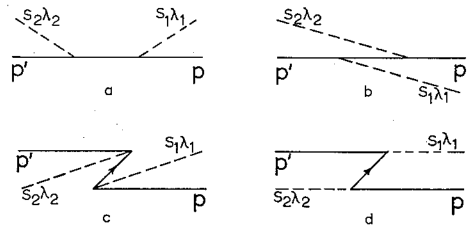

Fig. 14. The four second order diagrams contributing to Compton scattering.

In our non-relativistic case ($\mu \ll 1$, $\omega_{s_1} \ll m$) we have

$$\omega_{s_2}/\omega_{s_1} \simeq (1 + \omega_{s_1}(1 - \cos\theta)/m)^{-1} = 1 + \mathrm{O}(\omega_{s_1}/m) \qquad (5.9)$$

where θ is the angle between $\boldsymbol{k}_{s_1}$ and $\boldsymbol{k}_{s_2}$. We find

$$\{\langle \boldsymbol{p}'; s_2\lambda_2 |S| \boldsymbol{p}; s_1\lambda_1\rangle\}_{a+b} \simeq -2\pi i\delta(E(\boldsymbol{p}') + \omega_{s_2} -$$
$$- E(\boldsymbol{p}) - \omega_{s_1})\, \delta_{Kr}(\boldsymbol{p}' + \boldsymbol{k}_{s_2} - \boldsymbol{p} - \boldsymbol{k}_{s_1})$$
$$\tilde{N}_{p'}{}^{\frac{1}{2}}\tilde{N}_{p}{}^{\frac{1}{2}} \exp[-\tfrac{1}{4}\textstyle\sum_{s\lambda}^{\varpi} (\sigma^2{}_{p's\lambda} + \sigma^2{}_{ps\lambda})](\boldsymbol{\mu}, \boldsymbol{a}_{s_1\lambda_1})(\boldsymbol{\mu}, \boldsymbol{a}_{s_2\lambda_2})m^{-1}\mathrm{O}(1). \quad (5.10)$$

The two diagrams fig. 14c and 14d contribute

$$\{\langle \boldsymbol{p}'; s_2\lambda_2 |S| \boldsymbol{p}; s_1\lambda_1\rangle\}_{c+d} \simeq$$
$$\simeq -2\pi i\delta(E(\boldsymbol{p}') + \omega_{s_2} - E(\boldsymbol{p}) - \omega_{s_1})\, \delta_{Kr}(\boldsymbol{p}' + \boldsymbol{k}_{s_2} - \boldsymbol{p} - \boldsymbol{k}_{s_1})$$
$$\tilde{N}_{p'}{}^{\frac{1}{2}}\tilde{N}_{p}{}^{\frac{1}{2}} \exp[-\tfrac{1}{4}\textstyle\sum_{s\lambda}^{\varpi} (\sigma^2{}_{p's\lambda} + \sigma^2{}_{ps\lambda})](\boldsymbol{a}_{s_1\lambda_1}, \boldsymbol{a}_{s_2\lambda_2})/(-2m). \qquad (5.11)$$

It is easily seen that the contribution of (5.10) is unimportant as compared with the contribution of (5.11). The ratio is proportional to μ^2, and vanishes if $\mu = 0$. From (5.11) we find in second order (i.e. replacing the factor $\tilde{N}_{p'}^{\frac{1}{2}}\tilde{N}_{p}^{\frac{1}{2}} \exp[-\frac{1}{4}\sum_{s\lambda}^{\varpi}(\sigma^2_{p's\lambda}+\sigma^2_{ps\lambda})]$ by 1) the cross section

$$(\mathrm{d}\sigma/\mathrm{d}\Omega)_{(2)} = r_0^2(\boldsymbol{\varepsilon}_{s_1\lambda_1}, \boldsymbol{\varepsilon}_{s_2\lambda_2})^2 \tag{5.12}$$

where $r_0 = e^2/m$ is the classical electron radius and where $\boldsymbol{\varepsilon}_{s_1\lambda_1}$ and $\boldsymbol{\varepsilon}_{s_2\lambda_2}$ are polarization vectors ($\boldsymbol{a}_{s\lambda} = 2e(\pi/\Omega\omega_s)^{\frac{1}{2}}\,\boldsymbol{\varepsilon}_{s\lambda}$). Formula (5.12) is the well known Thomson formula.

The factor $\exp[-\frac{1}{4}\sum_{s\lambda}^{\varpi}(\sigma^2_{p's\lambda}+\sigma^2_{ps\lambda})]$ in (5.11) vanishes due to the infrared divergent summation (compare with (2.8)). If we take into account all radiative corrections to Compton scattering, we will find again (compare with (3.4)) that the complete matrix element $\langle \boldsymbol{p}'; s_2\lambda_2 |S| \boldsymbol{p}, s_1\lambda_1\rangle$ vanishes.

Let us now discuss the radiative corrections. From the fact that the diagrams of fig. 14*a* and 14*b* give vanishing contributions in the low-energy limit we conclude that it is unnecessary to consider radiative corrections to them: corrections from high energy virtual photons are of relative order α after renormalization while corrections in the infrared region have the same degree of divergence as the corresponding corrections to the diagrams of fig. 14*c* and 14*d*. This means that among others the following classes of diagrams are irrelevant:

1. Diagrams without any shaded area. They are constructed by adding only soft photon lines to the diagrams of fig. 14*a* and 14*b*.

2. Diagrams of the type fig. 15*a* and 15*b*. They are a simple extension of fig. 14, in which the two vertices and the internal electron line are corrected with shaded areas. All such corrections together only give rise to an additional factor $\tilde{N}_{p'}^{-\frac{1}{2}}\tilde{N}_{p}^{-\frac{1}{2}}$ in (5.10) cancelling $\tilde{N}_{p'}^{\frac{1}{2}}\tilde{N}_{p}^{\frac{1}{2}}$.

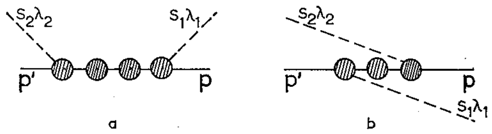

Fig. 15. Shaded area corrections to the vertices and internal electron line of fig. 14*a* and 14*b*.

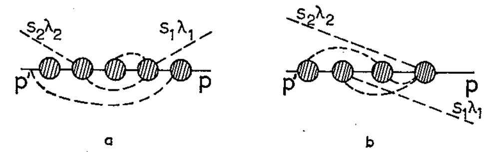

Fig. 16. Radiative corrections to fig. 14*a* and 14*b* in which shaded areas are connected by means of soft photon lines.

3. Diagrams of the type fig. 16*a* and 16*b* in which some shaded areas are connected by means of soft photon lines

From this it is seen that relevant diagrams should have the property that the two external photon lines are attached to one and the same shaded area. It is therefore convenient, in analogy with section 3, to define the basic diagrams for Compton scattering as being the diagrams of the kind given in fig. 17 (two external photon lines and two external electron lines attached to one and the same shaded area). The diagrams of fig. 14*c* and 14*d* are the simplest examples of basic diagrams.

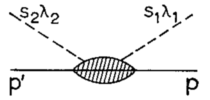

Fig. 17. Basic diagram for Compton scattering.

A relevant diagram for Compton scattering in the low-energy limit can now be either a basic diagram or a radiative correction to a basic diagram. In analogy with section 3 we find that relevant corrections to a basic diagram come from virtual soft photon lines which overlap the shaded area in fig. 17. All these soft photon lines together give rise to a factor

$$\sum_{m=0}^{\infty} \{\tfrac{1}{2} \sum_{s\lambda}^{\varpi} \sigma_{p's\lambda}\, \sigma_{ps\lambda}\}^m/m!$$

in the matrix element for the basic diagram (compare with (3.2)). It should be noted, however, that some basic diagrams are irrelevant in the low-energy limit. For instance basic diagrams in which the external photons are attached to closed loops are certainly irrelevant (see above the conventional proof of Thirring's theorem). The same holds for basic diagrams in which the whole electron path is straight, because they are corrections $O(\alpha)$ to the irrelevant diagrams of fig. 14*a* and 14*b*.

Let the total contribution of all basic diagrams be

$$\{\langle \boldsymbol{p}'; s_2\lambda_2 |S| \boldsymbol{p}; s_1\lambda_1\rangle\}_{basic} =$$
$$= -2\pi i\, \delta(E(\boldsymbol{p}') + \omega_{s_2} - E(\boldsymbol{p}) - \omega_{s_1})\, \delta_{Kr}(\boldsymbol{p}' + \boldsymbol{k}_{s_2} - \boldsymbol{p} - \boldsymbol{k}_{s_1})\, \tilde{N}_{p'}^{\frac{1}{2}} \tilde{N}_{p}^{\frac{1}{2}}$$
$$\exp[-\tfrac{1}{4}\textstyle\sum_{s\lambda}^{\varpi}(\sigma^2_{p's\lambda} + \sigma^2_{ps\lambda})]\, \mathscr{B}(\boldsymbol{p}'; s_2\lambda_2; \boldsymbol{p}, s_1\lambda_1) \qquad (5.13)$$

(compare with (3.1)). In order to get the contribution of all radiative corrections to Compton scattering in the low-energy limit of the external photons we have to multiply (5.13) with the factor

$$\sum_{m=0}^{\infty} \{\tfrac{1}{2} \sum_{s\lambda}^{\varpi} \sigma_{p's\lambda}\sigma_{ps\lambda}\}^m/m!.$$

We then find for the total contribution of all relevant diagrams in this limit

$$\langle \boldsymbol{p}'; s_2\lambda_2 |S| \boldsymbol{p}; s_1\lambda_1\rangle = -2\pi i\, \delta(E(\boldsymbol{p}') + \omega_{s_2} - E(\boldsymbol{p}) - \omega_{s_1})\delta_{Kr}(\boldsymbol{p}' + \boldsymbol{k}_{s_2} - \boldsymbol{p} - \boldsymbol{k}_{s_1})$$
$$\tilde{N}_{p'}^{\frac{1}{2}} \tilde{N}_{p}^{\frac{1}{2}}\, \mathscr{B}(\boldsymbol{p}', s_2\lambda_2; \boldsymbol{p}, s_1\lambda_1) \exp[-\tfrac{1}{4} \textstyle\sum_{s\lambda}^{\varpi} (\sigma_{p's\lambda} - \sigma_{ps\lambda})^2]. \qquad (5.14)$$

The function $\tilde{N}_{p'}^{\frac{1}{2}} \tilde{N}_{p}^{\frac{1}{2}}\, \mathscr{B}(\boldsymbol{p}', s_2\lambda_2; \boldsymbol{p}, s_1\lambda_1)$ involves the infrared cut off $\bar{\omega}$. Expressed in terms of the renormalized mass and charge it has a finite limit when the ultraviolet cut off tends to infinity. The expression (5.14) vanishes due to the infrared behaviour of the exponential. Only in the case $\boldsymbol{p}' = \boldsymbol{p}$ (this holds in particular when the external photons have zero momentum, which is the situation considered by Thirring) does the expression not vanish. Barring this unrealistic situation we simply find that taking into account all radiative corrections leads to a vanishing cross section, which obviously contradicts Thirring's theorem.

We now remark, however, that the arguments of Thirring can be succesfully applied to low-energy Compton scattering if one restricts all virtual photons to energies $\omega > \bar{\omega}$. This restriction cannot affect the arguments because renormalization is an ultraviolet matter. When this restriction is made the vanishing exponential factor in (5.14) is absent and one can write for small ω_{s_1}, ω_{s_2} and $\boldsymbol{p}$,

$$\tilde{N}_{p'}{}^{\frac{1}{2}}\tilde{N}_{p}{}^{\frac{1}{2}}\,\mathscr{B}(\boldsymbol{p}', s_2\lambda_2; \boldsymbol{p}, s_1\lambda_1) = \\ = (\boldsymbol{a}'_{s_1\lambda_1}, \boldsymbol{a}'_{s_1\lambda_2})/(-\,2m')\; F(\bar{\omega}; \boldsymbol{p}', s_2\lambda_2; \boldsymbol{p}, s_1\lambda_1), \quad (5.15)$$

where the factor $(\boldsymbol{a}'_{s_1\lambda_1}, \boldsymbol{a}'_{s_2\lambda_2})/(-\,2m')$ (involving the renormalized chargs and mass e' and m') according to (5.11) and (5.12) gives rise to the Thomsoe cross section. According to Thirring's proof the function $F(\bar{\omega}; \boldsymbol{p}', s_2\lambda_2$n $\boldsymbol{p}, s_1\lambda_1)$ for $\boldsymbol{p} = 0$ and $\omega_{s_1} = \omega_{s_2} = 0$ can be put equal to 1 neglecting th; small contribution from the frequency region $(0, \bar{\omega})$ to the charge and mase renormalization. Indeed, if $\bar{\omega} \ll m$, charge and mass renormalization are not affected by the restriction on the virtual photons. If $0 < \omega_{s_1}, \omega_{s_2} \ll m$ the function $F(\bar{\omega}; \boldsymbol{p}', s_2\lambda_2; \boldsymbol{p}, s_1\lambda_1)$ can be put equal to 1 in a whole $\bar{\omega}$-region, as will be seen later on. According to (5.15) one finds for the complete theory without the restriction $\omega > \bar{\omega}$ on the virtual photons

$$\langle \boldsymbol{p}', s_2\lambda_2\,|S|\,\boldsymbol{p}, s_1\lambda_1\rangle = \\ = -\,2\pi i\;\delta(E(\boldsymbol{p}') + \omega_{s_2} - E(\boldsymbol{p}) - \omega_{s_1})\;\delta_{Kr}\,(\boldsymbol{p}' + \boldsymbol{k}_{s_2} - \boldsymbol{p} - \boldsymbol{k}_{s_1}) \\ (\boldsymbol{a}'_{s_1\lambda_1}, \boldsymbol{a}'_{s_2\lambda_2})/(-\,2m')\;F(\bar{\omega}; \boldsymbol{p}', s_2\lambda_2; \boldsymbol{p}, s_1\lambda_1)\;\exp[-\tfrac{1}{4}\,\Sigma_{s\lambda}^{\bar{\omega}}(\sigma_{p's\lambda} - \sigma_{ps\lambda})^2] \quad (5.16)$$

which leads to the (vanishing) cross section

$$\mathrm{d}\sigma(\boldsymbol{p}', s_2\lambda_2; \boldsymbol{p}, s_1\lambda_1)/\mathrm{d}\Omega = r_0'^2(\boldsymbol{\varepsilon}_{s_1\lambda_1}, \boldsymbol{\varepsilon}_{s_2\lambda_2})^2\,|F(\bar{\omega}; \boldsymbol{p}', s_2\lambda_2; \boldsymbol{p}, s_1\lambda_1)|^2 \\ \exp[-\,\tfrac{1}{2}\,\Sigma_{s\lambda}^{\bar{\omega}}(\sigma_{p's\lambda} - \sigma_{ps\lambda})^2]\;\delta_{Kr}(E(\boldsymbol{p}') + \\ + \omega_{s_2} - E(\boldsymbol{p}) - \omega_{s_1})\;\delta_{Kr}(\boldsymbol{p}' + \boldsymbol{k}_{s_2} - \boldsymbol{p} - \boldsymbol{k}_{s_1}), \quad (5.17)$$

where $r_0' = e'^2/m'$ is the classical electron radius in terms of the renormalized mass and charge.

We now want to take into account all multiple Compton processes in which in addition to the soft but observable photon with momentum $\boldsymbol{k}_{s_2}$, soft photons are emitted with a total energy $\leq \Delta\varepsilon$. We then redefine the cross section for Compton scattering in a way quite analogous to the corresponding case for bremsstrahlung (section 4) and we find, summing over all unobservable sets of photons $\{n_{s\lambda}\}$, by the same method as in section 3 and 4

$$\Sigma'_{\{n_{s\lambda}\}}(\mathrm{d}\sigma(\boldsymbol{p}', s_2\lambda_2, \{n_{s\lambda}\}; \boldsymbol{p}, s_1\lambda_1)/\mathrm{d}\Omega) = r_0'^2(\boldsymbol{\varepsilon}_{s_1\lambda_1}, \boldsymbol{\varepsilon}_{s_2\lambda_2})^2$$
$$|F(\bar\omega; \boldsymbol{p}', s_2\lambda_2; \boldsymbol{p}, s_1\lambda_1)|^2\, \delta_{Kr}(E(\boldsymbol{p}')+\omega_{s_2}-E(\boldsymbol{p})-\omega_{s_1})\, \delta_{Kr}(\boldsymbol{p}'+\boldsymbol{k}_{s_2}-\boldsymbol{p}-\boldsymbol{k}_{s_1})$$
$$\exp[-\alpha C(\boldsymbol{p}', \boldsymbol{p}) \ln \bar\omega/\Delta\varepsilon], \tag{5.18}$$

the difference with (5.17) being that the infrared divergence in the exponential is now removed (compare with (4.10)).

With the aid of the expression (5.18) (i.e. with the redefined cross section for Compton scattering) we are now able to discuss the effect of radiative corrections in the low-energy limit. First of all we have to realize that this 'low-energy limit' for the two external photons has to be taken in the sense that those photons are observable, i.e. that their energies verify $\Delta\varepsilon < \omega_{s_1}, \omega_{s_2} \ll m$. In the rest system of the incoming electron we find for (5.18)

$$\Sigma'_{\{n_{s\lambda}\}}(\mathrm{d}\sigma(\boldsymbol{k}_{s_1} - \boldsymbol{k}_{s_2}, s_2\lambda_2, \{n_{s\lambda}\}; \boldsymbol{o}, s_1\lambda_1)/\mathrm{d}\Omega) =$$
$$= r_0'^2(\boldsymbol{\varepsilon}_{s_1\lambda_1}, \boldsymbol{\varepsilon}_{s_2\lambda_2})^2\, |F(\bar\omega; \boldsymbol{k}_{s_1} - \boldsymbol{k}_{s_2}, s_2\lambda_2; \boldsymbol{o}, s_1\lambda_1)|^2 \exp[-\alpha C(\boldsymbol{k}_{s_1} - \boldsymbol{k}_{s_2}, \boldsymbol{o})$$
$$\ln \bar\omega/\Delta\varepsilon]. \tag{5.19}$$

The exponential factor in (5.19) can be replaced by 1 if the following inequalities hold

$$\bar\omega \exp[(\alpha C(\boldsymbol{k}_{s_1} - \boldsymbol{k}_{s_2}, \boldsymbol{o}))^{-1}] \gg \Delta\varepsilon \gg \bar\omega \exp[-(\alpha C(\boldsymbol{k}_{s_1} - \boldsymbol{k}_{s_2}, \boldsymbol{o}))^{-1}]. \tag{5.20}$$

This is found by observing that $\alpha \ll 1$ and $C(\boldsymbol{k}_{s_1} - \boldsymbol{k}_{s_2}, \boldsymbol{o}) = \mathrm{O}(\omega_{s_1}{}^2/m^2)$. The low-energy cut off $\bar\omega$, however, is an artificial quantity, verifying $\bar\omega \ll m$. When $\Delta\varepsilon$ is fixed and verifies

$$m \gg \Delta\epsilon \gg m \exp[-(\alpha C(\boldsymbol{k}_{s_1} - \boldsymbol{k}_{s_2}, \boldsymbol{o}))^{-1}] \tag{5.21}$$

which is the case in actual experiments (note that $\exp[-(\alpha C(\boldsymbol{k}_{s_1} - \boldsymbol{k}_{s_2}, \boldsymbol{o}))^{-1}] \ll \exp(-137] \approx 10^{-60})$, we find a whole $\bar\omega$-region in which the exponential factor in (5.19) can be taken equal to 1, i.e. in which the inequalities (5.20) hold. This region is $m \gg \bar\omega \gg m \exp[-(\alpha C(\boldsymbol{k}_{s_1} - \boldsymbol{k}_{s_2}, \boldsymbol{o}))^{-1}]$. Since the left-hand side of (5.19) cannot depend on $\bar\omega$, we conclude that $|F(\bar\omega; \boldsymbol{k}_{s_1} - \boldsymbol{k}_{s_2}, s_2\lambda_2; \boldsymbol{o}, s_1\lambda_1)|^2$ is independent of $\bar\omega$ for $m \gg \bar\omega \gg m \exp[-(\alpha C(\boldsymbol{k}_{s_1} - \boldsymbol{k}_{s_2}, \boldsymbol{o}))^{-1}]$. In that region we can write $|F(\bar\omega; \boldsymbol{k}_{s_1} - \boldsymbol{k}_{s_2}, s_2\lambda_2; \boldsymbol{o}, s_1\lambda_1)|^2 \simeq 1 + \mathrm{O}(\alpha C(\boldsymbol{k}_{s_1} - \boldsymbol{k}_{s_2}, \boldsymbol{o}) \ln m/\bar\omega) \simeq 1$ if $\omega_{s_1}, \omega_{s_2} \ll m$ and we find for (5.19), under the condition (5.21)

$$\Sigma'_{\{n_{s\lambda}\}}\, \mathrm{d}\sigma(\boldsymbol{k}_{s_1} - \boldsymbol{k}_{s_2}, s_2\lambda_2, \{n_{s\lambda}\}; \boldsymbol{o}, s\lambda)/\mathrm{d}\Omega = r_0'^2(\boldsymbol{\varepsilon}_{s_1\lambda_1}, \boldsymbol{\varepsilon}_{s_2\lambda_2})^2 \tag{5.22}$$

which is the Thomson formula in terms of renormalized mass and charge. This result provides us with a new realistic formulation of the Thirring theorem, applicable to observable cross sections. It is satisfactory that in our derivation the low-energy cut off $\bar\omega$, which plays an important role in the definition of basic diagrams, can be chosen quite arbitrarily in the region

$$m \gg \bar\omega \gg m \exp[-(\alpha C(\boldsymbol{k}_{s_1} - \boldsymbol{k}_{s_2}, \boldsymbol{o}))^{-1}].$$

Acknowledgements. The author is greatly indebted to Professor L. Van Hove, who suggested the present investigation, for his most valuable advice and criticism throughout this work.

REFERENCES

1) Van Haeringen, W., Physica **26** (1960) 289.
2) Jauch, J. M. and Rohrlich, F., Helv. Phys. Acta **27** (1954) 613.
3) Thirring, W., Phil. Mag. **41** (1950) 1193.
4) Bloch, F. and Nordsieck, A., Phys. Rev. **52** (1937) 54.
5) Nakanishi, N., Progr. Theor. Phys. **19** (1958) 159.
6) Yennie, D. R. and Suura, H., Phys. Rev. **105** (1957) 1378.
7) Jauch, J. M. and Rohrlich, F., *The theory of photons and electrons*. Addison-Wesley Publ. Comp., Inc. p. 246, 247.
8) Dyson, F. J., Phys. Rev. **75** (1949) 1736.

MOTIVERING EN SAMENVATTING

De quantum electrodynamica, die een beschrijving geeft van de effecten optredende bij de wisselwerking tussen electronen, positronen en fotonen is momenteel zonder twijfel één van de meest succesvolle veldentheorieën. Zij geeft onder meer met grote precisie de hyperfijnstructuur van het waterstofspectrum, alsook het anomale magnetische moment van het electron. Toch kan de quantum electrodynamica niet als een volledig bevredigende theorie worden beschouwd. In de eerste plaats niet omdat men bij de berekeningen die steeds met storingstheorie worden uitgevoerd, te maken heeft met divergenties die optreden t.g.v. de hoge frequentiegebieden (de zogenaamde ultraviolet divergenties). Deze divergenties vereisen een speciaal soort behandeling, die zeer gecompliceerd is en berust op de idee dat divergenties van deze soort opgevat dienen te worden als renormalisatie van massa en lading. In de tweede plaats heeft men echter te maken met divergenties t.g.v. het lage frequentiegebied der fotonen (men noemt ze infrarood divergenties). De divergenties van deze soort treden op t.g.v. het feit dat de rustmassa van het foton nul is. Ze zijn van een geheel andere klasse dan de eerstgenoemde divergenties en kunnen dan ook niet worden geëlimineerd met behulp van een renormalisatieprocedure.

Het fundamentele werk van Bloch en Nordsieck [1]) *) heeft het nodige inzicht verschaft in de aard van de moeilijkheden in het infrarode frequentie gebied. Deze auteurs behandelen een vereenvoudigd model van de electrodynamica, waarin effecten van creatie en annihilatie van electron-positron paren alsmede terugstooteffecten van het electron verwaarloosd zijn. Zij merken op dat dit model een goede vervanging is van de complete theorie als men zich beperkt tot lage frequenties der e.m. trillingen. Het model kan exact worden opgelost en een eenvoudige toepassing op verstrooiing van electronen aan een zwakke potentiaal leert dat zulk een verstrooiingsproces noodzakelijkerwijs vergezeld gaat van emissie van niet waarneembare zwakke straling bestaande uit oneindig veel quanta met een zeer kleine totale energie. Dit verschijnsel blijkt de fysische verklaring te geven van de in de mathematische behandeling optredende infrarood divergenties. Of deze conclusie nu ook zonder meer geldig is voor de volledige electro-

*) Zie de literatuurlijst op pag. 16.

dynamica wordt door het werk van Bloch en Nordsieck wel zeer waarschijnlijk gemaakt, het vereist echter nog een expliciete bewijsvoering.

Dit probleem werd rigoureus aangepakt door Jauch en Rohrlich [2]. In een relativistisch covariante behandeling waarin Feynman diagrammen een fundamentele rol spelen breiden zij het werk van Bloch en Nordsieck uit in die zin dat rekening gehouden wordt met stralingseffecten van alle golflengten. Deze behandeling liet echter verscheidene vraagpunten over, die een verdere bestudering van het infrarood probleem vereisten. De geldigheidsgrenzen van Jauch en Rohrlich's resultaten werden door Lomon [3] in geding gebracht. Nakanishi [4] merkte op dat bepaalde diagrammen waarin zachte (d.w.z. laag energetische) fotonlijnen verbonden zijn met inwendige lijnen zonder rechtvaardiging zouden zijn verwaarloosd in Jauch en Rohrlich's behandeling. Yennie en Suura [5] gaven een soortgelijke beschouwing als Jauch en Rohrlich waaruit iets duidelijker blijkt waarop het wegvallen van infrarode divergenties tengevolge van zwakke virtuele fotonen enerzijds en zwakke reele fotonen anderzijds berust.

Behalve deze vraagpunten en verschillen in beschrijving is er nog een probleem betreffende Compton verstrooiing in de niet relativistische limiet (verstrooiing van zachte fotonen aan langzame electronen), waarin de moeilijkheden worden veroorzaakt door divergenties in het infrarode frequentiegebied. Een theorema van Thirring [6] zegt dat alle waarneembare stralingscorrecties in de niet relativistische limiet moeten verdwijnen. Overige stralingscorrecties geven slechts aanleiding tot renormalisatie van lading en massa in de z.g. Thomson formule die de laagste orde werkzame doorsnede geeft voor Compton verstrooiing in de niet relativistische limiet. Echter, een berekening in eindige orde blijkt in strijd met dit theorema. Zij b.v. vermeld de berekening van Brown en Feynman [7] van de werkzame doorsnede in zesde orde in de lading.

Met het oog op alle genoemde moeilijkheden werd het probleem van de i.r. divergenties aan een nieuw onderzoek onderworpen. De hierbij gevolgde methode sluit nauw aan bij die van Bloch en Nordsieck.

In het eerste hoofdstuk wordt het model van Bloch en Nordsieck uitvoerig bestudeerd. Daarbij worden de exacte uitdrukkingen voor de één-electron toestanden gevonden met behulp van diagrammen, een manier die een duidelijk inzicht geeft in de verwaarlozingen die in het model zijn verwezenlijkt. Nagegaan wordt dat deze verwaarlozingen (paar- en terugstooteffecten) zijn toegestaan in het lage frequentiegebied. Daarbij wordt ingegaan op de ook voor lage foton energie aanwezige gevolgen van paar creatie- en annihilatie, te weten vacuumpolarisatie en ladingsrenormalisatie. De gebruikte diagramtechniek is gebaseerd op het niet-covariante storingsformalisme van Van Hove [8] en Hugenholtz [9], en blijkt zeer geschikt te zijn voor de behandeling van problemen in het i.r. frequentiegebied.

In het tweede hoofdstuk worden twee verstrooiingsprocessen bestudeerd met het oog op de eraan verbonden infrarode aspecten. Dit wordt gedaan in het kader van de complete theorie, waarbij dus geen beperking is opgelegd aan het frequentiegebied. Ten eerste wordt behandeld bremsstrahlung, waarbij het uitwendige veld waaraan electronen verstrooid worden, in eerste Born benadering behandeld wordt. De verstrooiing wordt bestudeerd met behulp van de *S*-matrix, waarbij gebruik wordt gemaakt van bovengenoemde niet-covariante diagramtechniek. Deze techniek localiseert zeer duidelijk alle van belang zijnde infrarode effecten. Het blijkt dat een bevredigende beschrijving van bremsstrahlung kan worden verkregen met een enigszins gewijzigde definitie van overgangswaarschijnlijkheid. Deze definitie sluit nauw aan bij het door Bloch en Nordsieck gevonden resultaat, dat zulk een proces vergezeld gaat van emissie van een oneindig aantal aantal quanta met kleine totale energie. Als tweede proces wordt bestudeerd Compton verstrooiing in de niet relativistische limiet. Het theorema van Thirring blijkt slechts houdbaar in zijn bovenvermelde vorm, als men werkt met een gewijzigde definitie van de werkzame doorsnede (een wijziging analoog aan die bij het bremsstrahlung proces). Het is bevredigend dat deze nieuwe formulering van het theorema van Thirring niet langer in strijd is met bovenvermelde berekening van Brown en Feynman.